POLYOXOMETALATES

Open Access
REVIEW ARTICLE

Oxygen donor protection of atomically precise metal nanoclusters

Jia-Jing Lan[1], Yao-Yao Lian[2], Ya-Nan Yang[1], Wen-Ting Liu[1], Zong-Jie Guan[2] ✉, Kuan-Guan Liu[3] ✉, Qiao-Hua Wei[1] ✉, Zhen Lei[1] ✉, and Quan-Ming Wang[4] ✉

[1] *Fujian Provincial Key Laboratory of Advanced Inorganic Oxygenated Materials, College of Chemistry, Fuzhou University, Fuzhou 350108, China*
[2] *Department of Chemistry, College of Chemistry and Chemical Engineering, Hunan University, Changsha 410082, China*
[3] *Ningxia Key Laboratory for Photovoltaic Materials, School of Materials and New Energy, Ningxia University, Yinchuan 750021, China*
[4] *Department of Chemistry, Engineering Research Center of Advanced Rare Earth Materials (Ministry of Education), Tsinghua University, Beijing 100084, China*

Cite This: *Polyoxometalates*, **2026**, *5*, 9140113

Read Online

ABSTRACT: Over the past decades, metal nanoclusters have emerged as a novel class of highly attractive materials, owing to their atomic-level precision, complete homogeneity, and intriguing properties such as luminescence and catalytic activity. Typically, a metal nanocluster consists of a metal core surrounded by surface ligands. While the metal core plays a crucial role, it is increasingly recognized that surface ligands are far more than mere stabilizing agents. Compared to classical organic ligands such as thiolates and phosphines, oxygen (O) donors—including carboxylates, sulfonates, phosphinates, and phosphonates—have long been known but remain underestimated. Notably, O donors exhibit diverse coordination modes, making them particularly promising candidates for generating novel architectures. Moreover, O donors are highly effective in introducing chirality, luminescence, and other functionalities into metal nanoclusters. Many of these donors are also inexpensive, readily available, stable under ambient conditions, and easy to handle. In this review, we systematically summarize the development of O-donor protection in atomically precise cionage metal nanoclusters, with a particular emphasis on the structures of surface motifs associated with O donors. We also briefly survey the reported properties of clusters featuring O-donor protection. We hope this review will draw greater attention to O donors as ligands for nanoclusters, given their promising potential in generating novel structures and properties, particularly in coinage-metal nanoclusters.

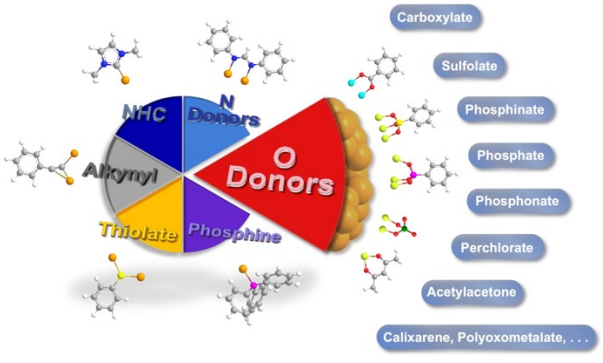

KEYWORDS: oxygen donor ligands, coinage metal nanocluster, coordination

1 Introduction

Atomically precise coinage-metal nanoclusters have attracted considerable attention over the past few decades [1]. In terms of size and structure, metal nanoclusters typically span the sub-nanometer to nanometer scale. However, owing to their molecular nature, they possess well-defined molecular structures and uniform sizes, in contrast to conventional nanomaterials. Many metal nanoclusters also exhibit promising luminescent and catalytic properties that rival those of larger metal nanoparticles and nanocrystals [2–5]. These unique characteristics have made metal nanoclusters indispensable for advancing nanochemistry. However, direct observation of their molecular structures—especially for larger clusters—offers valuable insights into the aggregation of metal atoms and the subsequent growth into nanoparticles [6–8]. More importantly, metal nanoclusters can be considered miniature analogs of nanoparticles, providing excellent platforms for exploring structure–property relationships at both atomic and nanoscale levels.

Typically, a metal nanocluster consists of a metal core surrounded by surface ligands. Although the metal core is fundamentally important, it is increasingly recognized that surface ligands play roles far beyond merely stabilizing the nanocluster. This is because metal–ligand interactions are crucial in shaping the overall structures and properties of these clusters. Among these, the application of phosphine [9–13] and thiolate [14–17] ligands was initially established and remains the subject of extensive study. Over the past two decades, considerable efforts have been devoted to developing new organic ligands to further advance coinage-metal nanoclusters. As a result, clusters protected by alkynyl [18–21], N-

Received: December 12, 2025; **Revised:** December 31, 2025
Accepted: January 5, 2026

✉Address correspondence to Zong-Jie Guan, zjguan@hnu.edu.cn; Kuan-Guan Liu, liukuanguan@nxu.edu.cn; Qiao-Hua Wei, qhw76@fzu.edu.cn; Zhen Lei, zhenlei@fzu.edu.cn; Quan-Ming Wang, qmwang@tsinghua.edu.cn

https://doi.org/10.26599/POM.2026.9140113

heterocyclic carbene (NHC) [22–24], and nitrogen (N) donor ligands [25–27] etc., were reported. Meanwhile, oxygen (O) donor ligands—including carboxylates, phosphonates, and sulfonates—are well known, yet their roles in the broader framework of metal nanocluster ligands remain somewhat underestimated.

According to the classical hard–soft acid–base (HSAB) theory, coinage-metal atoms (Au, Ag, and Cu) are generally classified as soft acids, showing a preference for forming strong bonds with soft bases such as phosphines and thiolates [28]. In contrast, hard-base ligands—particularly those containing O donors—typically interact only weakly with relatively hard copper or silver atoms. For example, in the pioneering example of O-donor protection for atomically precise metal nanoclusters reported in 1976, ^{t}BuOH molecules were observed on the cluster surface [29]. To improve the affinity of O donors toward metal atoms, it is beneficial to use negatively charged, multidentate O-donor ligands. As early as 1985, bidentate carboxylates carrying a −1 charge were identified as suitable candidates for stabilizing metal nanoclusters [30]. Since then, the family of O-donor ligands has expanded rapidly to include new members such as phosphonates and sulfonates, and recent studies have reported novel nanocluster structures stabilized by these ligands. Notably, during the 2000s, Mak and coworkers reported a series of copper and silver nanoclusters and investigated their associated properties [31–35]. O-donor ligands have been shown to offer several distinct advantages. First, they exhibit diverse coordination modes, making them promising candidates for the construction of novel architectures. Second, they serve as effective carriers for introducing chirality, luminescence, and other functionalities into metal nanoclusters. Furthermore, most O-donor ligands are cost-effective, readily available, stable under ambient conditions, and easy to handle. More recently, calixarenes and polyoxometalates have emerged as novel classes of O-donor ligands, providing enhanced stability and additional functionalities to metal nanoclusters. As a result, it is now widely recognized that O-donor ligands represent an independent category of organic ligands with considerable design flexibility.

This review provides a systematic summary of the development of O-donor protection in atomically precise metal nanoclusters, with a particular focus on the structures of surface motifs associated with O donors. The properties reported for clusters stabilized by O-donor ligands are also briefly discussed. We hope this review will draw greater attention to O donors as versatile ligands for nanoclusters, given their demonstrated potential in enabling new structures and properties, particularly in coinage-metal nanoclusters.

2 Structures stabilized by O-donor ligands

Although O-donor ligands have not yet been systematically explored for their ability to stabilize coinage-metal nanoclusters, an increasing number of such structures have been reported. These include, but are not limited to, nanoclusters protected by carboxylates, sulfonates, phosphinates, phosphonates, newly developed calixarenes and polyoxometalates, and other related ligands. Here, we categorize the documented structures by ligand type, summarize their characteristic coordination motifs, and provide a comprehensive discussion of selected representative clusters.

2.1 Metal nanoclusters with carboxylates

Carboxylates, as one of the most common classes of O-donor ligands, are widely used in the formation of metal complexes. In most metal nanoclusters stabilized by O-donor ligands, carboxylate groups typically coordinate to metal atoms in staple-like or higher-denticity modes, ranging from chelating to bridging binding motifs (Scheme 1). They can also interact with auxiliary ligands to further stabilize the metal core, resulting in diverse structural configurations. In this section, we highlight several representative compounds that exhibit particularly intriguing coordination motifs or structural features.

For coinage metals, carboxylates predominantly form coordination bonds with silver and copper, typically introduced via metal salts. A commonly cited example is CF_3CO_2Ag [3, 36–40]. The first coinage-metal cluster protected by the $CF_3CO_2^-$ ligand, $Cu_4(CF_3CO_2)_4(EtC{\equiv}C)_2$ (**Cu_4**), was synthesized by Adams in 1989 (Fig. 1(a)) [36]. In this cluster, each of the four $CF_3CO_2^-$ ligands is coordinated to two Cu atoms along the edges of the tetrahedral Cu_4 core, forming motif 1d. Later, in 2000, Fenske and coworkers reported a mixed-valence silver cluster, $[Ag(^tBuNH_2)_2]_4[Ag(^tBuNH_2)(^tBuN{=}CHCH_3)]_2[Ag_{12}(CF_3CO_2)_{14}]$ (designated as **Ag_{12}**, Fig. 1(b)) [37]. Similar to the **Cu_4** cluster, the $CF_3CO_2^-$ ligands coordinate to silver atoms in motif 1d. More recently, Wang's group reported a novel one-dimensional (1D) chain structure, $[Au_7Ag_9(dppf)_3(CF_3CO_2)_7BF_4]_n$ (referred to as **Au_7Ag_9-1D**; dppf denotes 1,10-bis(diphenylphosphino)ferrocene), derived from classical M_{13} clusters ($Au@Au_6Ag_6$) [40]. In this M_{13} cluster, the Au atoms are protected by three dppf ligands, while the Ag atoms are stabilized by $CF_3CO_2^-$ ligands. Some $CF_3CO_2^-$ ions also coordinate with additional silver atoms, promoting the linkage of clusters into a 1D superstructure, as shown in Fig. 1(c). In total, the $CF_3CO_2^-$ ligands in combination with silver atoms form four distinct motifs. Specifically, ligands in motifs 1a and 1d chelate only the silver atoms in the M_{13} core, whereas those in motifs 1e and 1f also bind to external silver atoms, thereby generating the 1D cluster-based chain.

Beyond $CF_3CO_2^-$, bicarboxylates can act as multidentate ligands. For example, in 2020, perfluoroglutarate (pfga) was used to stabilize coinage-metal nanoclusters [41]. Liu and colleagues reported an all-carboxylate-protected **Ag_8** cluster, $[Ag_8(pfga)_6]^{6-}$, representing the first superatomic silver nanocluster fully protected by carboxylates and featuring two free electrons (Fig. 1(d)). The chelating pfga

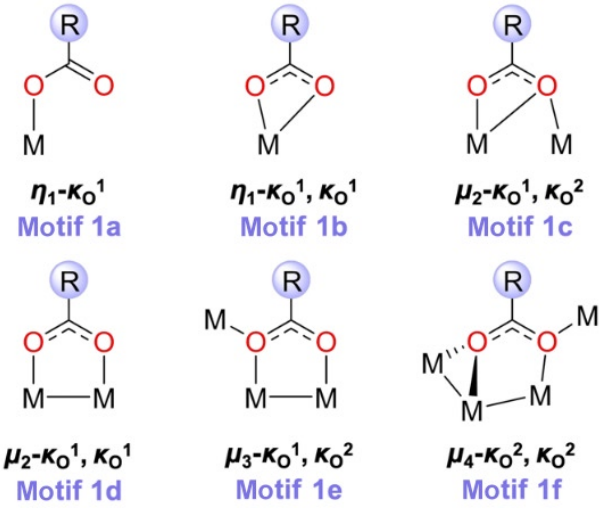

Scheme 1 Coordination modes of carboxylates on the surface of metal nanoclusters.

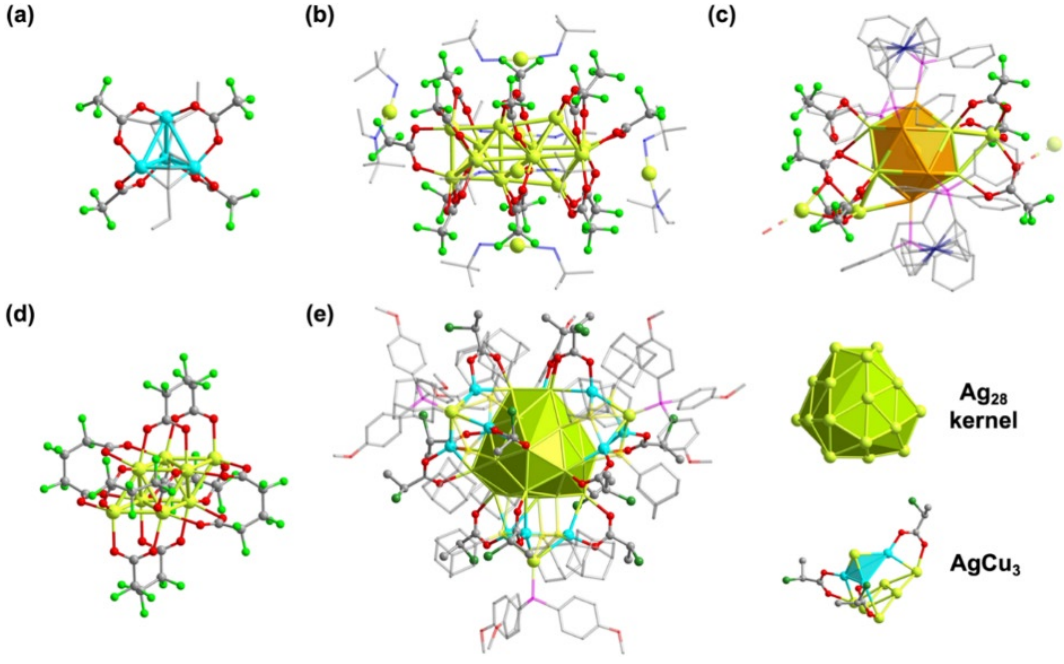

Figure 1 Structures of $\mathbf{Cu_4}$ (a), $\mathbf{Ag_{12}}$ (b), $\mathbf{Au_7Ag_9\text{-}1D}$ (c), $\mathbf{Ag_8}$ (d), and $\mathbf{Ag_{32}Cu_{12}}$ (e) (insert: structures of Ag_{28} kernel, $AgCu_3$ unit, and coordination mode of $Cl(CH_3)CHCO_2^-$), respectively. Hydrogen atoms are omitted for clarity. Color legend: C, gray; N, blue; O, red; F, yellowish green; P, purple; Cl, green; Fe, dark blue; Cu, turquoise; Ag, electric lime; Au, orange.

ligands adopt a μ_4-κ_O^1, κ_O^1, κ_O^1, κ_O^1 coordination mode, with each carboxylate interacting with silver atoms according to motif 1d. Chirality can also be introduced through the R group of carboxylates, occasionally rendering the two O donors inequivalent within a single structure. In 2021, Zhu and Wang reported a pair of chiral silver–copper clusters, ***R*-/*S*-$\mathbf{Ag_{32}Cu_{12}}$**, formulated as $[Ag_{32}Cu_{12}(R/S\text{-}Cl(CH_3)CHCO_2)_{12}(SAdm)_{12}(P(CH_3OPh)_3)_4]$ (SAdm = 1-adamantanethiolate) [42]. Here, the chiral *R*-/*S*-$Cl(CH_3)CHCO_2^-$ ligands connect silver and copper atoms via motif 1d, linking the $AgCu_3$ tetrahedral units to the central Ag_{28} kernel (Fig. 1(e)).

In addition to alkyl carboxylates, aromatic carboxylates—such as benzoate ($PhCO_2^-$)—are widely used in the synthesis of coinage-metal nanoclusters [43–51]. These ligands typically contain one or more aromatic rings, which can engage in intermolecular and intramolecular interactions, including π–π and σ–π interactions. In certain structural arrangements, Ag···π interactions have also been observed [52, 53]. Such interactions can considerably influence the structural formation and properties of metal nanoclusters, highlighting their importance in guiding cluster architecture and potential applications.

Wang's group reported a gold(I)–silver(I) cluster (**$\mathbf{CAu_6Ag_6}$**) featuring benzoates templated by a C^{4-} anion, characterized as $[(C)(Au\text{-}PPhpy_2)_6Ag_6(PhCO_2)_3](BF_4)_5$ [45]. In this cluster, the pyridine rings of the $PPhpy_2$ ligands and the $PhCO_2^-$ ligands co-protect the silver atoms on the surface of the $[(C)(Au\text{-}PPhpy_2)_6]^{2+}$ core (Fig. 2(a)). The $PhCO_2^-$ ligands adopt motif 1d, identical to that observed in the **$\mathbf{Cu_{20}}$** cluster, $[Cu_{20}(PhSe)_{12}(PPh_3)_2(PhCO_2)_6]$, reported by Shen and coworkers (Fig. 2(b)) [46]. Through the use of molybdate anions, Sun's group reported two silver clusters $[Mo_8O_{28}@Ag_{50}(^tPrS)_{24}(PhCO_2)_{18}(CH_3CN)_2)]\cdot 4CH_3CN$ (**$\mathbf{Ag_{50}}$**) [47] and $[Ag_{10}@(MoO_4)_7@Ag_{60}(^tBuC_6H_4S)_{33}(mbc)_{18}(DMF)(H_2O)_2]$ (**$\mathbf{Ag_{70}}$**) (mbc = 4-MeO-$PhCO_2^-$) [49] co-protected by benzoate and thiolate ligands. In **$\mathbf{Ag_{50}}$**, the benzoate ligands adopt motifs 1a, 1d, and 1e (Fig. 2(c)), while in **$\mathbf{Ag_{70}}$**, the mbc ligands adopt motifs 1d and 1e (Fig. 2(d)). The presence of three and two distinct coordination motifs in **$\mathbf{Ag_{50}}$** and **$\mathbf{Ag_{70}}$**, respectively, suggests that higher nuclearity and larger metal cores promote greater diversity in benzoate ligand coordination.

Beyond benzoate derivatives, carboxylates with extended aromatic systems have also been used to stabilize metal nanoclusters. In 2023, 9-anthracenecarboxylate (9-$AnCO_2^-$), featuring a multi-ring π-system, was used to protect silver nanoclusters. Liu and colleagues reported a series of isomorphic, carboxylate-protected superatomic **$\mathbf{Ag_{16}}$** nanoclusters mediated by phosphine and arsine ligands [50]. The metallic core can be viewed as an Ag_8 kernel surrounded by additional individual silver atoms. The Ag_8 kernel consists of a chair-shaped hexagonal ring with silver atoms positioned on both sides, interconnected via Ag–Ag interactions. The 9-$AnCO_2^-$ ligands stabilize the Ag_8 kernel while simultaneously coordinating to external silver atoms (Fig. 2(e)). For example, in $[Ag_{16}(Ph_3P)_8(9\text{-}AnCO_2)_{12}](OH)_2$, the 9-$AnCO_2^-$ ligands adopt motifs 1e and 1f. Each of the six ligands in motif 1e bridges three silver atoms: one at a vertex of the Ag_8 kernel, one on the Ag_6 ring, and one external silver atom. The remaining ligands in motif 1f connect two silver atoms on the Ag_6 ring and two external silver atoms.

Amino acids are among the most common chiral compounds in nature, valued for their biocompatibility and sustainability. Established synthetic methods allow the commercial availability of highly pure enantiomers. From a coordination chemistry perspective, deprotonated amino acids can be regarded as a specialized subclass of carboxylates, distinguished by an additional electron-donating amino group. Containing at least two oxygen atoms and one nitrogen atom, they represent a particularly attractive class of ligands for metal coordination. Metal nanoclusters stabilized by amino acids have been synthesized and exhibit novel structural and functional properties [54–58]. In 2021, Wang's research group reported a mixed-valence silver cluster co-protected by amino acid and alkyne ligands, $[Ag_{47}(L\text{-}/D\text{-valine})_{12}$

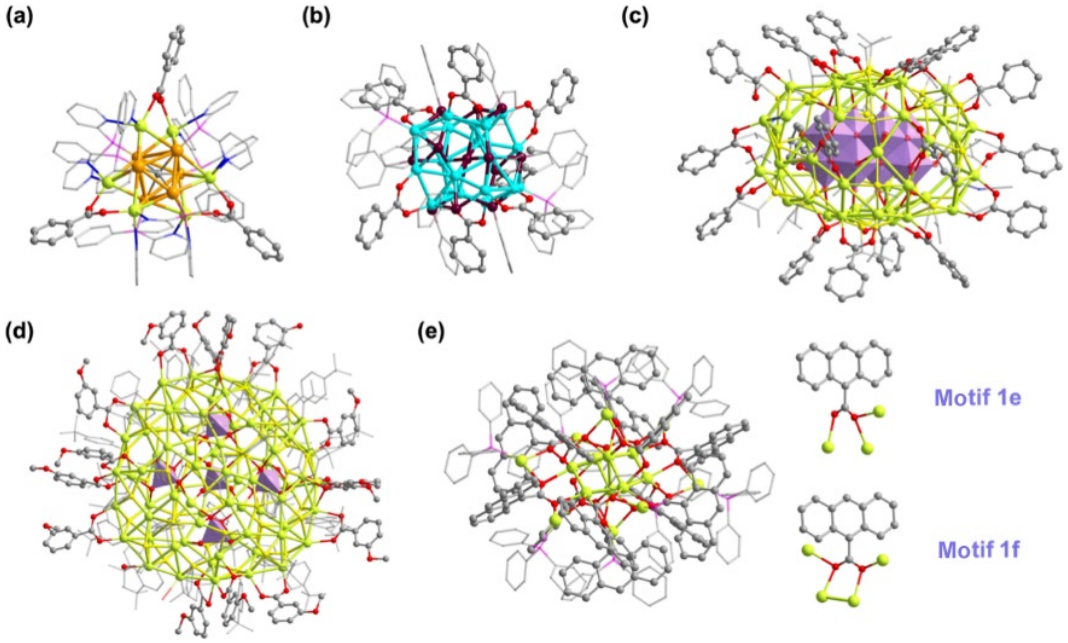

Figure 2 Structures of $\mathbf{CAu_6Ag_6}$ (a), $\mathbf{Cu_{20}}$ (b), $\mathbf{Ag_{50}}$ (c), $\mathbf{Ag_{70}}$ (d), and $\mathbf{Ag_{16}}$ (e) (insert: coordination modes of 9-$AnCO_2^-$), respectively. Hydrogen atoms are omitted for clarity. Color legend: C, gray; N, blue; O, red; P, purple; S, yellow; Cu, turquoise; Se, tyrian purple; Ag, electric lime; Au, orange.

$(C{\equiv}C^tBu)_{16}]BF_4$ (***L***-/***D***-$\mathbf{Ag_{47}}$, Fig. 3(a)) [55]. In this cluster, the surface amino acid ligands (*L*-/*D*-valine) adopt a μ_4-κ_O^1,κ_O^2,κ_N^1 coordination motif, reflecting the additional N-coordinated site. Interestingly, mass spectrometry and electronic structure analyses revealed that the $-NH_2$ group coordinated to silver atoms without deprotonation (Fig. 3(a)). Recently, they further reported chiral gold-silver nanoclusters, $[Au_7Ag_8(dppf)_3(L\text{-}/D\text{-proline})_5(C_4H_7NH_2^+CO_2^-)](BF_4)_2$, desigranted as ***L***-/***D***-$\mathbf{Au_7Ag_8}$, protected by amino acid and phosphine ligand (Fig. 3(b)) [56]. Unlike ***L***-/***D***-$\mathbf{Ag_{47}}$, the N sites of proline are not coordinated to the metals. Instead, only the carboxyl groups of proline bind to silver atoms, adopting motifs 1d and 1f (Fig. 3(b)). The uncoordinated N sites of the proline ligands, together with their cooperative interactions with the metal core, were leveraged to achieve excellent catalytic performance in asymmetric reactions using the $\mathbf{Au_7Ag_8}$ cluster.

In our survey, we found that monosubstituted monothiocarbonates ($ROC(=S)O^-$) have also been used in the synthesis of coinage-metal nanoclusters. These ligands are generated by replacing one oxygen atom in a carbonate group with a sulfur atom and can coordinate to cluster surfaces in a manner similar to carboxylates, representing a distinct subclass of carboxylate derivatives. In 2017, Liu and colleagues reported a copper(I) cluster, $Cu_{16}[CyOC(=S)O]_{16}$ ($\mathbf{Cu_{16}}$) [59]. In this cluster, the monothiocarbonate ligands coordinate to three or four copper atoms via μ_3-κ_O^1, κ_S^2 and μ_4-κ_O^1, κ_S^3 modes, respectively (Fig. 3(c)).

In summary, carboxylate ligands stabilize coinage-metal nanoclusters through two key features: They provide flexible, tunable coordination modes that support the formation of diverse and robust structures, and their organic backbones are readily

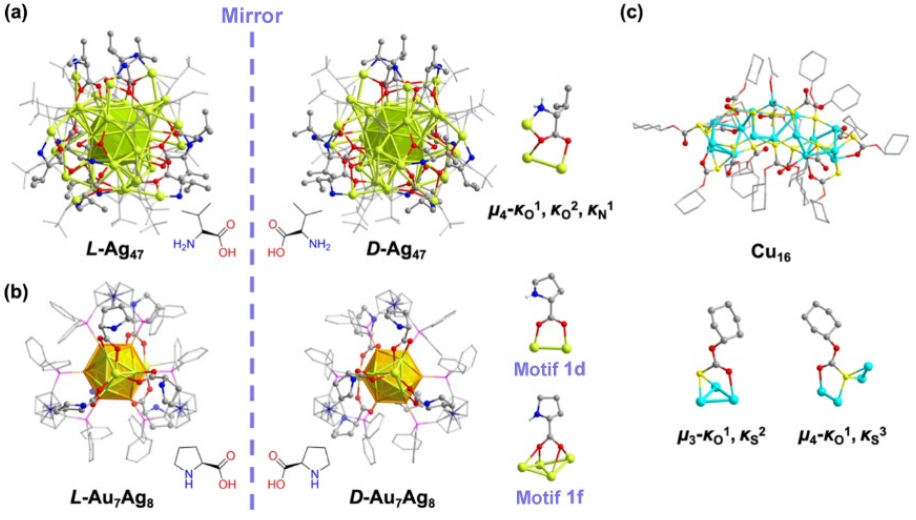

Figure 3 Structures of ***L***-/***D***-$\mathbf{Ag_{47}}$ (a) (insert: coordination mode of *D*-valine), ***L***-/***D***-$\mathbf{Au_7Ag_8}$ (b) (insert: coordination modes of *D*-proline), and $\mathbf{Cu_{16}}$ (c) (insert: coordination modes of $CyOC(=S)O^-$), respectively. Hydrogen atoms are omitted for clarity. Color legend: C, gray; N, blue; O, red; P, purple; S, yellow; Fe, dark blue; Cu, turquoise; Ag, electric lime; Au, orange.

functionalizable, allowing accurate control over the clusters' electronic and chiral properties.

2.2 Metal nanoclusters with sulfonates

Similar to carboxylates, sulfonates are anionic species carrying a single negative charge and have demonstrated considerable coordination capabilities with copper and silver ions in recent years. However, the presence of an additional O donor allows sulfonates to adopt a wider variety of coordination modes compared to carboxylates. Several of these motifs have been observed in coinage-metal nanoclusters to date (Scheme 2).

Several readily available alkyl and aryl sulfonate ligands have been widely used in coinage-metal nanocluster synthesis. For example, $CF_3SO_3^-$ can be introduced via the metal salt CF_3SO_3Ag, analogous to CF_3CO_2Ag. In 2000, Mak and colleagues reported a silver cage-based chain (**Ag_{7n}**) incorporating $CF_3SO_3^-$ ligands in motif 2i [60]. In this structure, each oxygen atom of the $CF_3SO_3^-$ ligand bridges two silver atoms (Fig. 4(a)). The $CF_3SO_3^-$ ligands play a critical role, acting not only as chelating and protective agents but also as essential linkers connecting silver cage units. Furthermore, Braunstein synthesized a Cu_3 cluster featuring a linear metal core, $[Cu_3(^tBu_2PC_{NHC}P^tBu_2)_2(CF_3SO_3)](CF_3SO_3)_2$, where $^tBu_2PC_{NHC}P^tBu_2$ denotes 1,3-bis(di-tert-butylphosphino)-imidazole-2-ylidene [61]. As shown in Fig. 4(b), it is evident that the $CF_3SO_3^-$ ligand in the **Cu_3** cluster adopts motif 2e.

Using the solvothermal synthetic method, Sun and coworkers successfully obtained two anion-templated silver clusters stabilized by aryl sulfonate ligands, namely $[Mo_7O_{24}@Ag_{41}(^iPrS)_{19}(p\text{-TOS})_{16}(CH_3OH)_4{\cdot}4CH_3OH]$ (**Ag_{41}**, *p*-TOS = p-toluene sulfonate) and $[Mo_4O_{14}(SO_4)]_2@Ag_{73}S_4(PhSO_3)_{17}(^tBuS)_{30}(SO_4)_3(H_2O)_4{\cdot}2H_2O$ (**Ag_{73}**) (Figs. 4(c) and 4(d)) [62, 63]. In **Ag_{41}**, the relatively smooth metal core surface is protected by *p*-TOS ligands, with each ligand coordinating to 2–4 silver atoms, forming motifs 2b, 2c, 2f, and 2g. In contrast, **Ag_{73}** exhibits a highly irregular core surface, likely because some phenyl sulfonate ligands penetrate the metal core. Therefore, the sulfonate ligands adopt a broader range of coordination modes, with motif 2h reaching a higher coordination number of 5.

Using chiral sulfonate ligands, *D*-/*L*-camphorsulfonic acid (*D*-/*L*-CSA), Zang's group reported enantiopure silver nanoclusters $[Ag_{12}(S^iPr)_6(D/L\text{-CSA})_6(\text{pyridine})_7(H_2O)]$ (***D*-/*L*-Ag_{12}**, Fig. 4(e)) [64]. In this cluster, the six CSA ligands adopt three distinct coordination motifs: 2a, 2b, and 2c. The combination of the chiral CSA ligands, the intrinsic properties of silver, and their mutual interactions collectively contribute to the remarkable circularly polarized luminescence (CPL) observed in these structures.

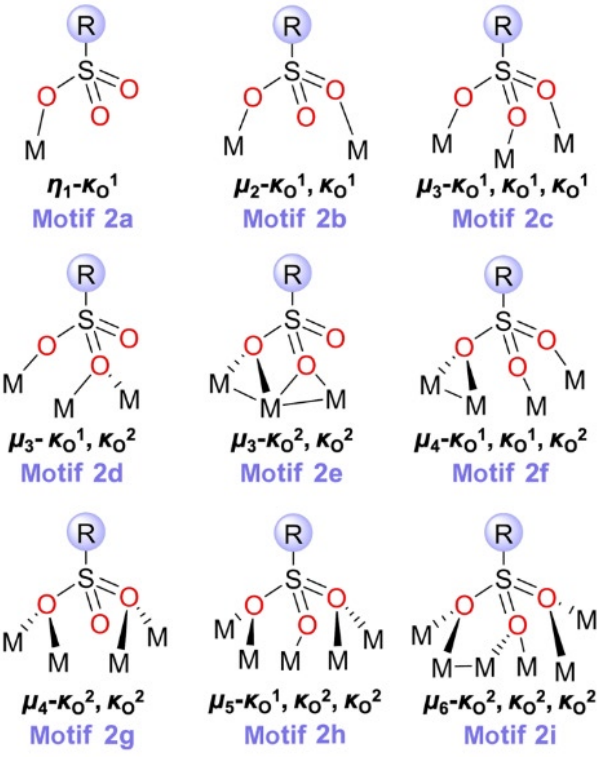

Scheme 2 Coordination modes of sulfonates on the surface of metal nanoclusters.

Overall, sulfonate ligands demonstrate diverse coordination modes with coinage metals, including both chelating and bridging arrangements, primarily owing to the presence of an additional O donor that expands their binding versatility.

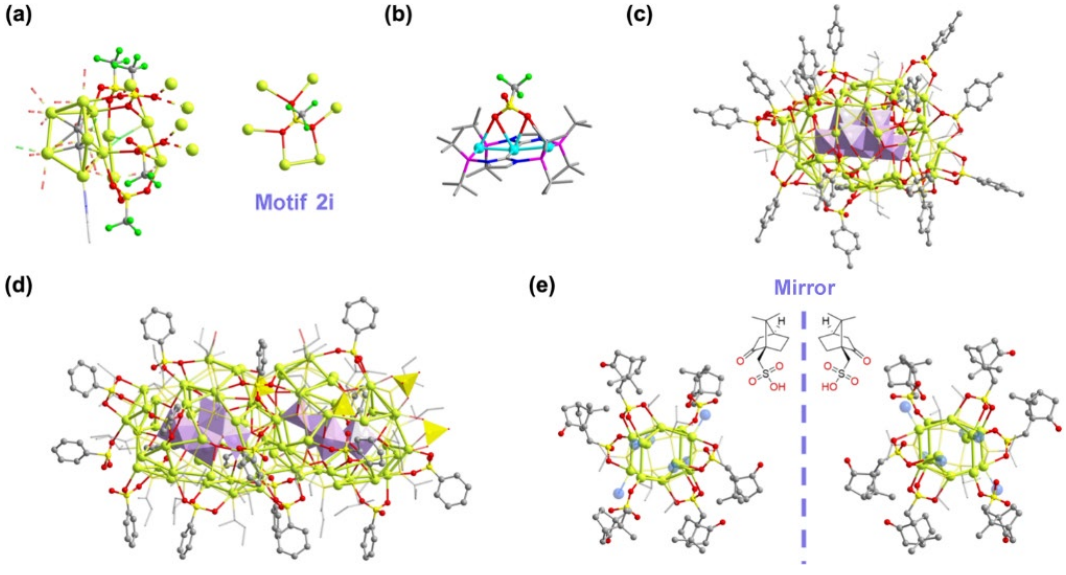

Figure 4 Structures of **Ag_{7n}** (a) (insert: coordination mode of $CF_3SO_3^-$), **Cu_3** (b), **Ag_{41}** (c), **Ag_{73}** (d), and ***D*-/*L*-Ag_{12}** (e), respectively. Hydrogen atoms are omitted for clarity. Color legend: C, gray; N, blue; O, red; F, yellowish green; P, purple; S, yellow; Cu, turquoise; Ag, electric lime.

2.3 Metal nanoclusters with phosphinates, phosphonates, and phosphates

Phosphinates, phosphonates, and substituted phosphates are structurally analogous to phosphoric acids. The proximity of phosphorus and sulfur in the periodic table accounts for the similar coordination behavior of these anionic species to sulfonates. Thus, they have shown promising capabilities as ligands for stabilizing metal nanoclusters in recent studies. Typically, a phosphinate has the general formula $R_2PO_2^-$ (e.g., diphenylphosphinate, $Ph_2PO_2^-$) and contains two alkyl or aryl groups directly bonded to the phosphorus atom. In contrast, a phosphonate features only one direct P–C bond, giving the general formula RPO_3^{2-} (e.g., tert-butylphosphonate, $^tBuPO_3^{2-}$). Substituted phosphates are derivatives of H_3PO_4 in which one or more hydrogen atoms are replaced by organic groups. When one or two hydrogens are replaced, forming mono- and disubstituted phosphates ($ROPO_3^{2-}$ or $(RO)_2PO_2^-$), these ligands retain the ability to coordinate to metal centers. Structurally, phosphinates ($R_2PO_2^-$) and disubstituted phosphates ($(RO)_2PO_2^-$) closely resemble carboxylates, whereas phosphonates (RPO_3^{2-}) and monosubstituted phosphates ($ROPO_3^{2-}$) are analogous to sulfonates. However, a notable distinction is that the P–O bond is longer than the S–O bond, enabling these ligands to accommodate coordination to a greater number of metal atoms. Furthermore, phosphonates and monosubstituted phosphates carry two negative charges, which enhances their affinity for metal atoms. These steric and electronic features contribute to a greater tendency for phosphinates, phosphonates, and phosphates to coordinate with more metal centers compared to carboxylates and sulfonates. Therefore, these ligands exhibit a wider variety of coordination modes and can achieve higher coordination numbers, reaching up to nine in certain metal nanocluster systems.

2.3.1 Phosphinates and disubstituted phosphates

Because both $R_2PO_2^-$ (e.g., diphenylphosphinate, $Ph_2PO_2^-$) and $(RO)_2PO_2^-$ (e.g., *R*-/*S*-1,1'-binaphthyl-2,2'-diylphosphate, *R*-/*S*-$BinapO_2PO_2^-$) contain two O atoms capable of metal coordination, these two classes are discussed together in a single subsection. Their coordination modes are shown in Scheme 3. Our analysis shows that, although the $-PO_2^-$ group has an atomic arrangement and number of donor atoms similar to $-CO_2^-$, ligands containing the $-PO_2^-$ moiety generally achieve higher coordination numbers, coordinating up to six metal atoms. This difference can be attributed to the larger atomic radius of phosphorus compared to carbon, which results in a P–O bond approximately 0.3 Å longer than a C–O bond in carboxylates, providing greater spatial flexibility for metal coordination.

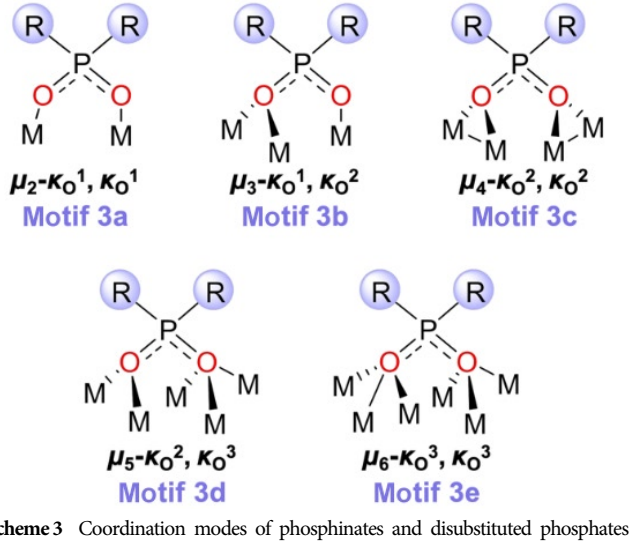

Scheme 3 Coordination modes of phosphinates and disubstituted phosphates on the surface of metal nanoclusters.

Among phosphinates, $Ph_2PO_2^-$ is the most commonly used ligand for constructing coinage-metal nanoclusters [65–67]. Wang and coworkers reported two silver nanoclusters protected by $Ph_2PO_2^-$, $[Ag_{21}(3,5\text{-}(MeO)_2\text{-}PhC{\equiv}C)_6(Ph_2PO_2)_{10}]SbF_6$ (**Ag_{21}-1**) and $[Ag_{21}(H_2BTCA)_3(Ph_2PO_2)_{10}]SbF_6$ (**Ag_{21}-2,** H_4BTCA = *p*-tert-butylthiacalix[4]arene) [65]. In **Ag_{21}-1**, the $Ph_2PO_2^-$ ligands adopt motifs 3a, 3b, 3c, and 3d, coordinating 2–5 silver atoms, respectively (Figs. 5(a) and 5(d)). The metal core of **Ag_{21}-1** consists of a central Ag_{13} icosahedron connected to two Ag_5 trigonal bipyramids via shared vertex atoms. Ligands in motifs 3b, 3c, and 3d bridge the Ag_{13} and Ag_5 units, stabilizing the entire metal core, while motif 3a chelates the Ag_5 units. These observations underscore the critical role of $Ph_2PO_2^-$ ligands in both stabilizing the cluster and facilitating the formation of high-nuclearity structures. In 2023, Liu and Morsali reported a 1D chain **Ag_{16n}** [66]. The coordination motif 3e was observed for the first time (Figs. 5(b) and 5(d)). In this motif, $Ph_2PO_2^-$ and $CF_3CO_2^-$ ligands together bridge the Ag_{16} units into a 1D chain, demonstrating that $Ph_2PO_2^-$ ligands can connect metal atoms to form higher-dimensional architectures and thereby enhance structural diversity.

R-/*S*-$BinapO_2PO_2^-$ is one of the few chiral phosphates featuring two O-coordinating sites. Recently, Chen's group reported chiral silver–copper cluster enantiomers, $[Ag_6Cu[CH(PPh_2)_3]_2(Ph_2NC_6H_4C{\equiv}C)_3(R\text{-}/S\text{-}BinapO_2PO_2)_3]ClO_4$ (***R*-/*S*-Ag_6Cu**) [67]. As shown in Figs. 5(c) and 5(d), the *R*-/*S*-$BinapO_2PO_2^-$ ligands in ***R*-/*S*-Ag_6Cu** connect all six silver atoms and are arranged exclusively in motif 3a. Meanwhile, the chirality of *R*-/*S*-$BinapO_2PO_2^-$ is transferred to the cluster with significant amplification, thereby influencing the CPL properties of this compound.

2.3.2 Phosphonates and monosubstituted phosphates

Both phosphonates and monosubstituted phosphates contain the same $-PO_3^{2-}$ moiety, providing three O-donor sites that can chelate more metal atoms than phosphinates (Scheme 4). Additionally, under certain synthetic or crystallization conditions, these ligands can be observed in their protonated forms ($-PO_3H^-$). When a proton is retained, the –OH group is capable of participating in hydrogen-bonding interactions, which introduce unique structural arrangements and chemical environments, further influencing the overall architecture of coinage-metal nanoclusters.

Phosphonates and monosubstituted phosphates have been widely used to construct high-nuclearity metal nanoclusters [68–71]. In 2017, Lu and Xie reported four silver clusters co-protected by functional phosphonates, thiolates, and alkynyl ligands [68]. Take **Ag_{33}** and **Ag_{48}** for example, $^tBuPO_3^{2-}$ and $^tBuPO_3H^-$ in $Ag_3S_3@Ag_{30}(^tBuC{\equiv}C)_6(^tBuS)_{12}(^tBuPO_3)(^tBuPO_3H)(hfac)_6(H_2O)_2$ (**Ag_{33}**) formed in motif 3j, and $^nBuPO_3^{2-}$ and $^nBuPO_3H^-$ in $S@Ag_{12}S_6@Ag_{36}(^tBuC{\equiv}C)_{12}(^tBuS)_{12}(^nBuPO_3)_2(^nBuPO_3H)_6$ (**Ag_{48}**) formed in motif 3l (Figs. 6(a) and 6(b)). In the **Ag_{48}** cluster, the central core consists of an $S@Ag_{12}S_6$ unit. Each O atom of the $^tBuPO_3^{2-}$ or $^tBuPO_3H^-$ ligands coordinates to one silver atom from this core. Additionally, two external silver atoms bind to the phosphonate ligands, forming motif 3l, which is characterized by a nonuple coordination to a single metal atom. The ligands adopt a semi-inserted, semichelating conformation, simultaneously

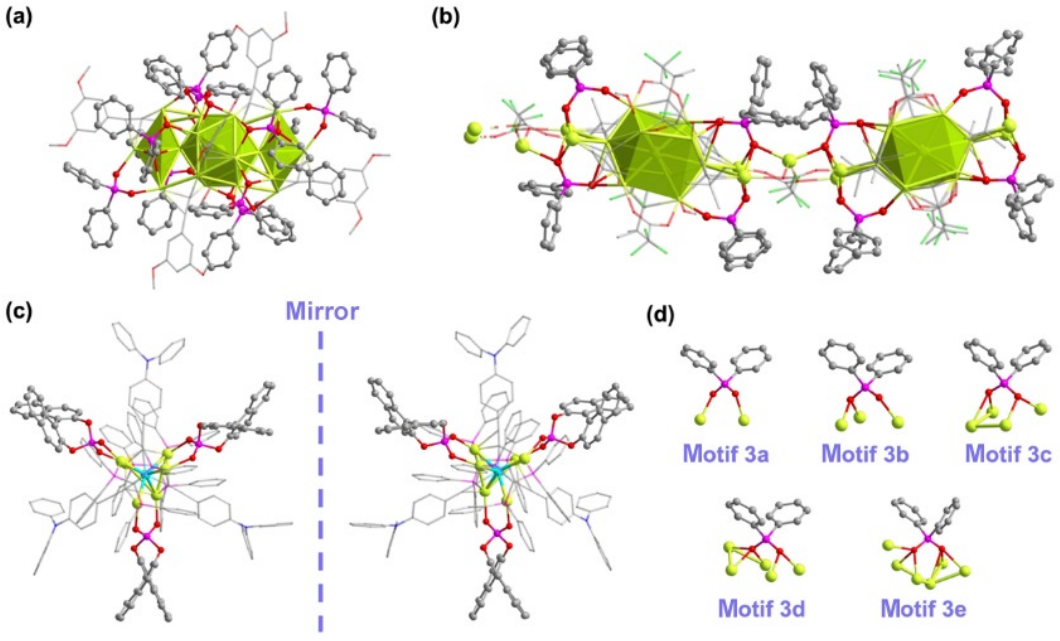

Figure 5 Structure of Ag_{21} (a), Ag_{16n} (b), and ***R***-/***S***-Ag_6Cu (c), respectively; (d) coordination modes of $Ph_2PO_2^-$ in Ag_{21} and Ag_{16n}. Hydrogen atoms are omitted for clarity. Color legend: C, gray; N, blue; O, red; F, yellowish green; P, purple; S, yellow; Cu, turquoise; Ag, electric lime.

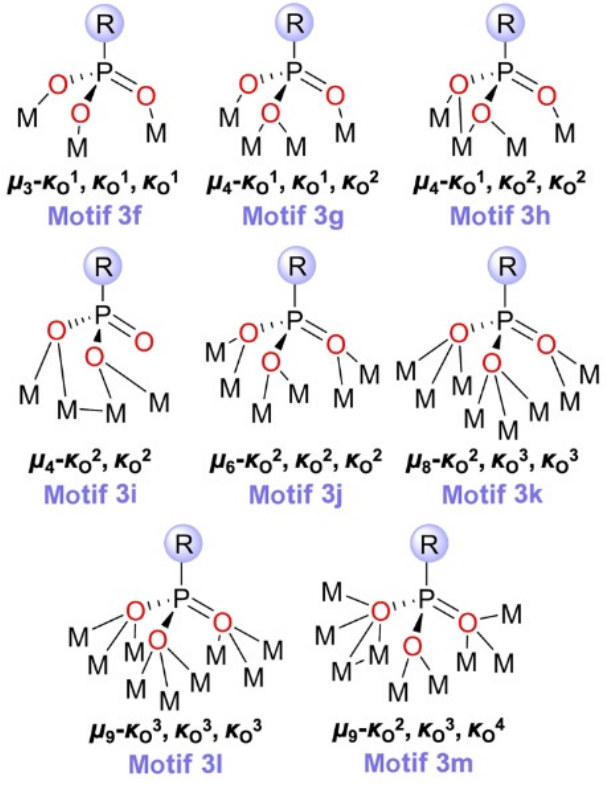

Scheme 4 Coordination modes of phosphonates and monosubstituted phosphates on the surface of metal nanoclusters.

stabilizing the central $S@Ag_{12}S_6$ core and chelating the outer-shell silver atoms. This demonstrates the ability of phosphonate ligands to "capture" metal atoms, providing opportunities for constructing structurally diverse coinage-metal nanoclusters.

In 2023, the same group reported another series of copper(I) clusters protected by alkynes and various phosphonate and monosubstituted phosphate ligands [69]. The phosphonate ligand $^tBuPO_3H_2$, and the phosphate ligands $PhOPO_3H_2$ ($PhOPO_3$ = phenyl phosphate), 1-$NaphOPO_3H_2$ (1-$NaphOPO_3$ = 1-naphthyl phosphate) were used in this work. These clusters were obtained as $[Na(PO_4)_6@Cu_{56}(^tBuPO_3)_6(^tBuC{\equiv}C)_{26}]F$ (**Cu_{56}-1**, Fig. 6(c)), $[Na(PO_4)_6@Cu_{56}(PhOPO_3)_6(^tBuC{\equiv}C)_{26}]F$ (**Cu_{56}-2**, Fig. 6(d)), and $[Na(PO_4)_6@Cu_{56}(1\text{-}NaphOPO_3)_6(^tBuC{\equiv}C)_{26}]F$ (**Cu_{56}-3**, Fig. 6(e)). Among the three closely related structures, the ligands in **Cu_{56}-1** adopt only motif 3g, whereas in **Cu_{56}-2/3**, an additional motif 3h is also observed (Fig. 6(f)). Replacing the $^tBuPO_3^{2-}$ ligands with $PhOPO_3^{2-}$ and 1-$NaphOPO_3^{2-}$ ligands leads to the formation of numerous strong intermolecular C–H–π interactions between adjacent clusters, which may influence the ligand coordination modes.

Overall, phosphorus-containing ligands—including phosphinates, phosphonates, and phosphates—provide enhanced steric flexibility and electron density owing to their longer P–O bonds and higher anionic charge compared with carboxylates and sulfonates. These features allow them to bind more metal atoms and achieve higher coordination numbers.

2.4 Metal nanoclusters with phenolate-type ligands

Phenolates carry a single negative charge and possess an extended aromatic system, which can enable strong interactions with metal atoms. However, phenolates are formally monodentate O donors and thus cannot effectively stabilize coinage-metal nanoclusters. Alternative strategies include introducing additional binding sites to create phenolate-like ligands or oligomerizing phenols or phenolates into calixarenes. As the number of coordination sites increases, the resulting coordination motifs become more diverse and differ substantially from those observed for classical carboxylates, sulfonates, phosphinates, and phosphonates (Scheme 5).

Disubstituted cyanurate ligands, containing both oxygen and multiple N donor sites, hold great potential as (co-)protecting ligands for coinage-metal nanoclusters. Sun and coworkers reported a nanocluster co-protected by diethylcyanurate and phosphine ligands, $[Ag_{22}(Cy\text{-}diEt)_9(dppm)_6Cl][NTf_2]_2Cl_2$ (**Ag_{22}**,

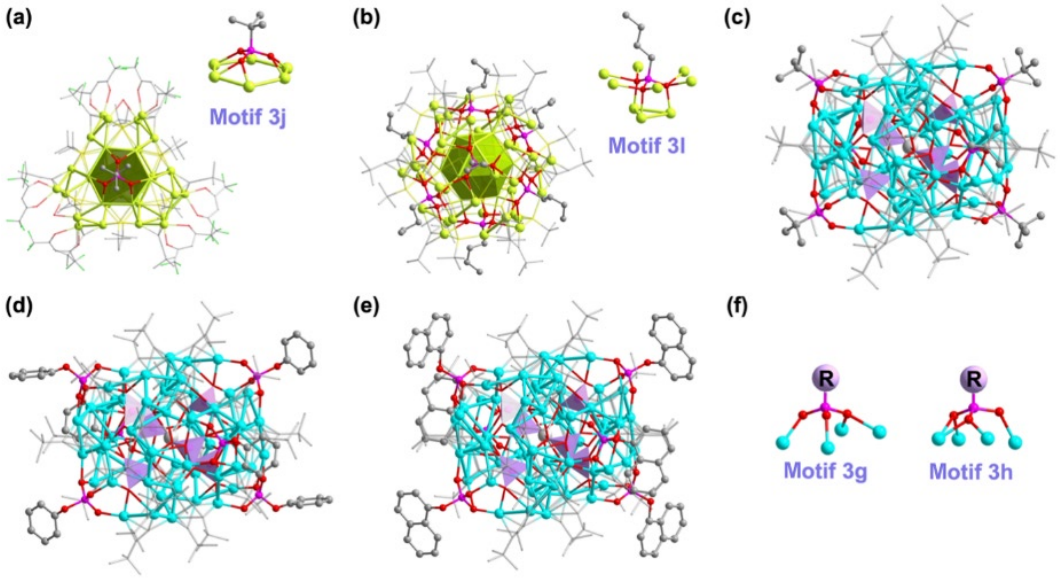

Figure 6 Structure of $\mathbf{Ag_{33}}$ (a) (insert: coordination mode of $^{t}BuPO_3^{2-}$), $\mathbf{Ag_{48}}$ (b) (insert: coordination mode of $^{n}BuPO_3^{2-}$), $\mathbf{Cu_{56}}$-**1** (c), $\mathbf{Cu_{56}}$-**2** (d), $\mathbf{Cu_{56}}$-**3** (e), and coordinating mode of RPO_3^{2-} in $\mathbf{Cu_{56}}$ (f), respectively. Hydrogen atoms are omitted for clarity. Color legend: C, gray; N, blue; O, red; P, purple; S, yellow; Na, light gray; Cu, turquoise; Ag, electric lime.

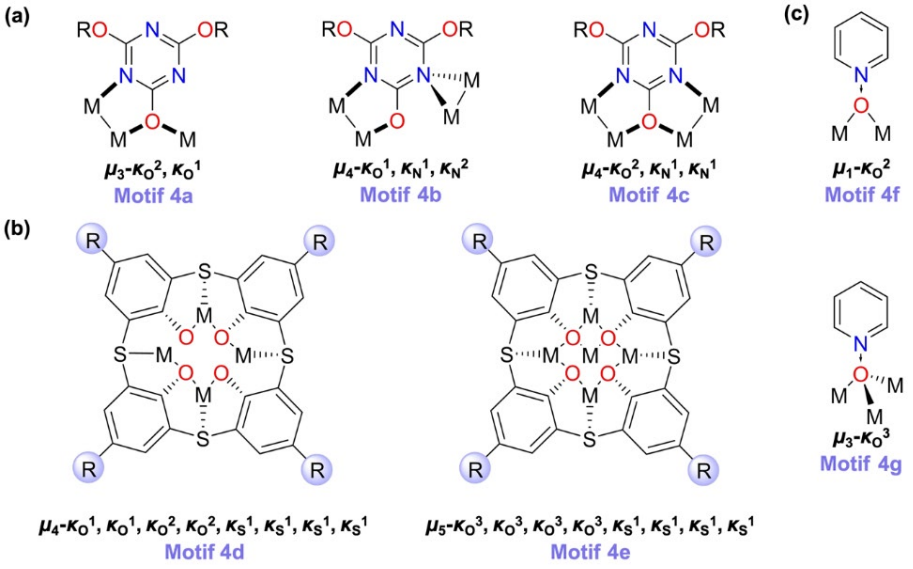

Scheme 5 Coordination modes of disubstituted cyanurates (a), calixarenes (b), and pyridine N-oxides (c) on the surface of metal nanoclusters.

CyH-diEt = diethylcyanurate; dppm = $Ph_2PCH_2PPh_2$, Fig 7(a)) [72]. During the synthesis of $\mathbf{Ag_{22}}$, the triallyl cyanurates are transformed into Cy-diEt, which coordinate to silver atoms on the cluster surface. Featuring phenolate-like O-donor sites alongside two neighboring N donors, Cy-diEt ligands adopt three distinct coordination motifs: 4a, 4b, and 4c.

Recently, calixarenes have emerged as a new class of ligands for the synthesis of coinage-metal nanoclusters. Structurally, calixarenes are oligomers of phenols and are characterized by their large spatial volume and conformational flexibility, which enable effective encapsulation and stabilization of the metal core. The characteristic calix-shaped cavity not only provides this encapsulation but also partially exposes certain metal atoms, creating confined reaction microenvironments at the cluster surface. This structural feature allows selective access of small molecules to the embedded metal sites, laying the foundation for catalytic applications. Calixarenes have been used in the synthesis of nanoclusters, particularly H_4BTCA [65, 73–80]. The first structurally characterized calixarene-protected metal nanocluster was reported by Wang and Lin in 2016 [73]. The $\mathbf{Ag_{35}}$ cluster ($[Ag_{35}(H_2BTCA)_2(BTCA)(^{t}BuC{\equiv}C)_{16}](SbF_6)_3$) is co-protected by $^{t}BuC{\equiv}C^-$ and $(H_nBTCA)^{4-n}$ ligands, with its structure shown in Fig. 7(b). In 2019, they constructed another $\mathbf{Ag_{34}}$ cluster ($[Ag_{34}(BTCA)_3(^{t}BuC{\equiv}C)_9(CF_3CO_2)_4(CH_3OH)_3]SbF_6$) with the same ligands (Fig. 7(c)) [74]. The abovementioned $\mathbf{Ag_{21}}$-**2** cluster ($[Ag_{21}(H_2BTCA)_3(O_2PPh_2)_6](SbF_6)$ is protected with $Ph_2PO_2^-$ and $(H_nBTCA)^{4-n}$ ligands (Fig. 7(d)) [65]. Two motifs of calixarene ligands were observed in the structure of $\mathbf{Ag_{35}}$, whereas only one motif was found in $\mathbf{Ag_{34}}$ and $\mathbf{Ag_{21}}$-**2**, respectively. For $(H_nBTCA)^{4-n}$, it adopts motif 4d when $n = 2$ and motif 4e when $n = 0$ (Fig. 7(f)). In comparison, the H_2BTCA^{2-} structure becomes distorted owing to hydrogen-bonding interactions between the proton-retaining hydroxyl group and an adjacent oxygen atom, as

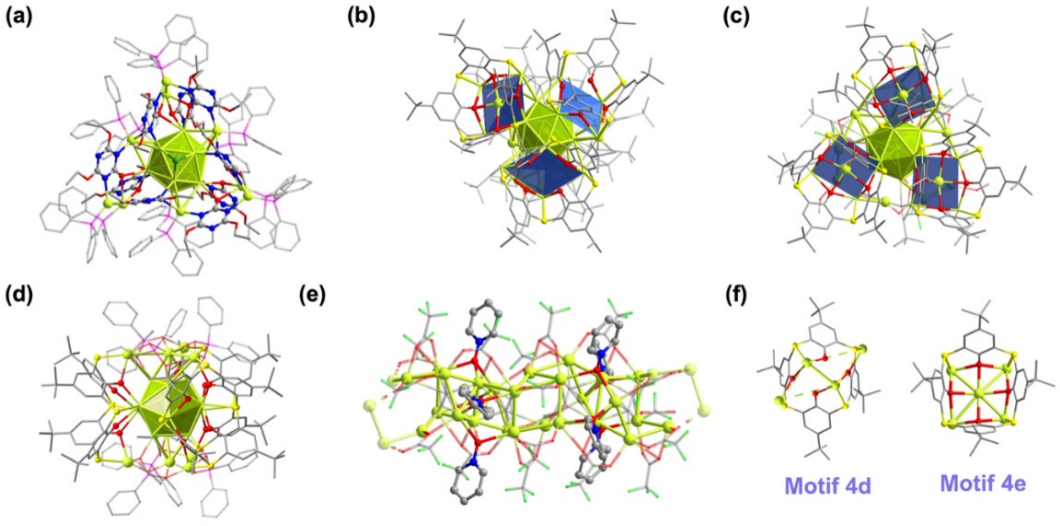

Figure 7 Structure of $\mathbf{Ag_{22}}$ (a), $\mathbf{Ag_{35}}$ (b), $\mathbf{Ag_{34}}$ (c), $\mathbf{Ag_{21}}$**-2** (d) and $\mathbf{Ag_{12}}_{n}$ (e); (f) coordinating motifs of H_2BTCA^{2-} and $BTCA^{4-}$. Hydrogen atoms are omitted for clarity. Color legend: C, gray; N, blue; O, red; F, yellowish green; P, purple; S, yellow; Ag, electric lime.

well as the lack of coordinating atoms within its cavity.

A special class of neutral ligands, pyridine N-oxide (pyO), which features an O-donor site, has been used in the construction of metal complexes. A pyO-coordinated 1D chain, $\mathbf{Ag_{12}}_{n}$, with the formula $[(Ag_2C_2)_2(AgCF_3CO_2)_8(pyO)_{3.5}]_n$, was reported by Mak and coworkers in 2006 (Fig. 7(e)) [81]. In this structure, O sites in pyO connect two or three metal atoms in motifs 4f and 4g.

Ligands derived from phenolates provide versatile strategies for stabilizing coinage-metal nanoclusters. By enabling multidentate coordination, structural confinement, and tailored surface environments, these ligands generate unique binding motifs, encapsulate metal cores, and present active sites, thereby facilitating applications in catalysis and molecular recognition.

2.5 Metal nanoclusters with other O-donor ligands

The family of O-donor ligands used for stabilizing metal nanoclusters extends beyond the described organic anions or molecules to include inorganic anions such as NO_3^- [58, 82–85] and ClO_4^- (Scheme 6) [45, 86]. These anions primarily act as counterions to balance the cluster charge but also possess weak coordinating abilities. Although NO_3^- and ClO_4^- lack additional functional groups, they can generate labile and unsaturated binding sites on the surfaces of metal nanoclusters, potentially serving as active centers for catalysis. Additionally, solvent molecules such as methanol and ethanol can act as labile ligands, providing a similar means to activate the cluster surface.

NO_3^- anions in nanoclusters can adopt versatile structural motifs on cluster surfaces by coordinating with 1–7 metal atoms. In 2014, Gao and Zang reported a silver cluster ($[Ag_{33}S_3(S^tBu)_{16}(CF_3CO_2)_9(NO_3)(CH_3CN)_2](NO_3)$, $\mathbf{Ag_{33}}$) and a cluster-based metal-organic layer ($[Ag_{31}S_3(S^tBu)_{16}(NO_3)_9]_n$, $\mathbf{Ag_{31}}_{n}$) [82]. In $\mathbf{Ag_{31}}_{n}$, eight NO_3^- ions adopt motifs 5b, 5c, 5f, and 5g, while the remaining nitrate anion adopts a 5j motif, serving as a surface template. Interestingly, upon cooling from 298 to 110 K, one oxygen atom of this NO_3^- shifts closer to an internal Ag_3 unit, concurrently transitioning to coordination mode 5k, which involves six silver atoms. A similar temperature-dependent behavior was observed in $\mathbf{Ag_{33}}$, where the surface-templating NO_3^- changed from motif 5i (coordinating with four silver atoms) at 298 K to motif 5l (coordinating with seven silver atoms) at 110 K (Fig. 8(a)). This temperature-induced change in coordination geometry provides valuable insights into the design and construction of coinage-metal nanoclusters. Other coordination modes, such as motifs 5a and 5h, were observed in $\mathbf{Ag_{38}}$, reported by Zheng's group in 2024 [85].

Similar to NO_3^-, ClO_4^- is a common anion in metal salts and can be used in the construction of coinage-metal nanoclusters [45, 86]. In the $\mathbf{CAu_6Ag_5}$ cluster reported by Wang in 2022, ClO_4^- ligands were used to stabilize silver atoms with motif 5m (Fig. 8(b)) [45]. When ClO_4^- coordinates with two metal atoms, two distinct motifs were observed in $\mathbf{Ag_{15}}$ and $\mathbf{Ag_{19}}$ clusters constructed by Orthaber in 2020 [86]. Motif 5o arises when only a single oxygen atom of ClO_4^- connects to two silver atoms, whereas motif 5n occurs when two oxygen atoms each connect to one silver atom.

Alcohols are commonly used as solvents in the synthesis of metal nanoclusters. Even without deprotonation, the oxygen atom in alcohol molecules can coordinate to metal centers, and nanoclusters with bound alcohol molecules are frequently observed. For example, an Au(I)-Ag(I) cluster $[Au_{12}Ag_{14}(C{\equiv}CPh)_{20}(mdppz)_4(CH_3OH)_8](BF_4)_6$ ($\mathbf{Au_{12}Ag_{14}}$, mdppz = 2-(3-methylpyrazinyl) diphenylphosphine) with eight coordinated MeOH molecules was synthesized (Fig. 8(c)) [87]. In this cluster, the methanol molecules bind to silver atoms without deprotonation. Similarly, in an Ag_{19} cluster reported by Liu and coworkers in 2022 [88], two methanol molecules were observed forming hydrogen bonds with neighboring $CF_3CO_2^-$ and $Ph_2PO_2^-$ ligands, thereby stabilizing the cluster framework. These observations highlight the importance of the hydrogen-bonding ability of O-donor ligands in shaping the structure of metal nanoclusters and enhancing their stability.

Another relatively underexplored class of O-donor ligands is acetylacetones. Acetylacetone itself lacks a conjugated system, but upon deprotonation, it forms a continuous, conjugated organic ligand with coordination ability, making it suitable for the construction of coinage-metal clusters [89, 90]. In 2018, Lu and Xie reported a series of silver clusters protected mainly by hexafluoroacetylacetone (hfac) and $^tBuC{\equiv}C^-$ ligand [90]. In $V_2O_7@Ag_{24}(^tBuC{\equiv}C)_{16}(hfac)_6$ ($\mathbf{Ag_{24}}$), hfac ligands effectively cap the edges of the cluster by adopting motifs 5q and 5r, thereby preventing the formation of polymeric structures (Fig. 8(d)). However, acetylacetone ligands have not yet been widely used or systematically explored in nanocluster synthesis.

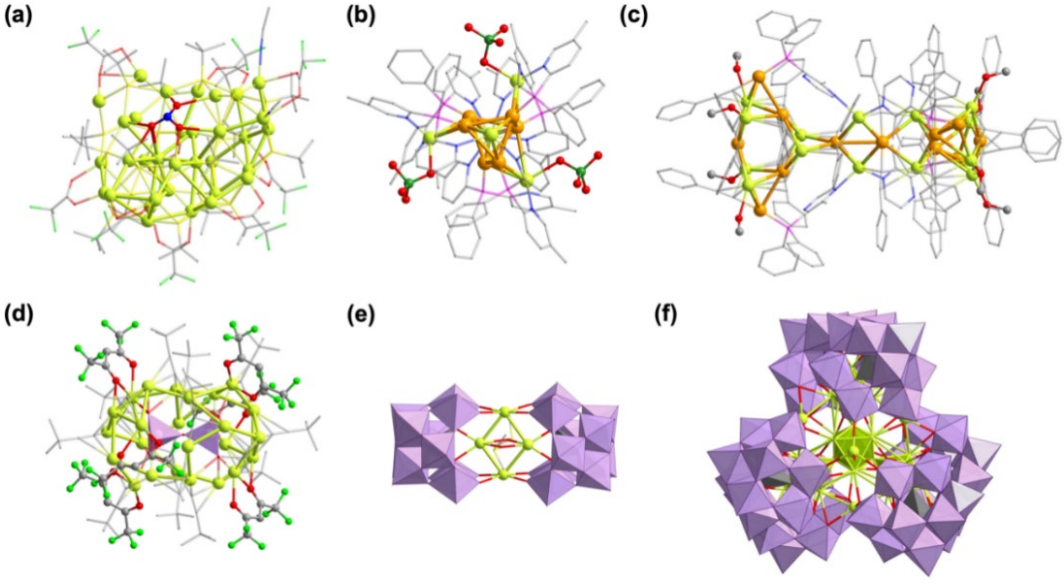

Figure 8 Structures of Ag_{33} (a), CAu_6Ag_5 (b), $Au_{12}Ag_{14}$ (c), Ag_{24} (d), Ag_4 (e), and Ag_{27} (f), respectively. Hydrogen atoms are omitted for clarity. Color legend: C, gray; N, blue; O, red; P, purple; S, yellow; Cl, green; Ag, electric lime; Au, orange.

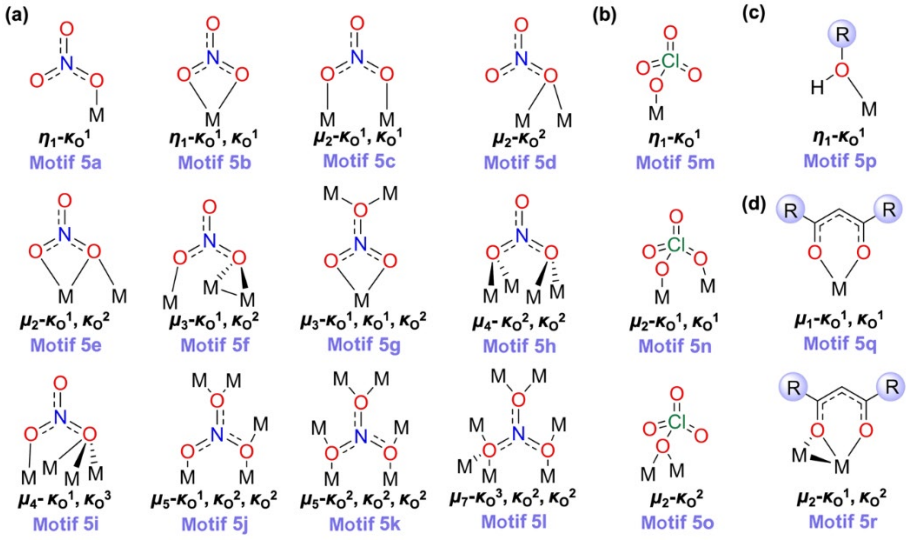

Scheme 6 Coordination modes of NO_3^- (a), ClO_4^- (b), alcohols (c), and acetylacetones (d) on the surface of metal nanoclusters.

Recently, polyoxometalates (POMs) have been identified as effective O-donor ligands for protecting coinage-metal nanoclusters [91–97]. POMs are a large family of anionic metal–oxygen clusters and exhibit high chemical stability compared to commonly used organic ligands. As early as 2012, Mizuno and coworkers synthesized a mixed-valence Ag_4 cluster [91]. The cluster is protected with $[SiW_{12}O_{40}]$, in which all oxygen atoms coordinate to silver atoms (Fig. 8(e)). In 2019, Suzuki et al. reported a mixed-valence Ag_{27} cluster, $[TBA_{16}(Me_2NH_2)_8H_5Ag_2[Ag_{27}(Si_2W_{18}O_{66})_3]$ (TBA = tetra-*n*-butylammonium, Fig. 8(f)) [92]. In this cluster, the O atoms coordinate to 1, 2, or 3 silver atoms, and the cluster core is built from four Ag_6 octahedra. The use of POMs for constructing coinage-metal nanoclusters is a promising yet challenging research direction.

3 Properties modulated with O-donor ligands

The formation of metal–oxygen interface structures leads to a wide range of novel configurations. Furthermore, the characteristics of specific O-donor ligands, combined with effects such as electron transfer resulting from their coordination to the metal, further influence the performance and properties of the clusters. Here, we present an overview of the key features observed in clusters stabilized by O-donor ligands (Fig. 9).

3.1 Catalysis

Metal nanoclusters have demonstrated considerable potential as catalysts for various organic and inorganic reactions. O-donor ligands, with their diverse geometries and coordination capabilities, can stabilize nanoclusters with unique electronic structures, making them particularly suitable for catalytic applications [56, 65, 91, 94–97]. In 2022, Wang's group reported two Ag_{21} clusters with a similar metal core and investigated their catalytic activities in the reduction of 4-nitrophenol (4-NP) [65]. They found that Ag_{21}-**1**, possessing four free electrons and an incomplete shell configuration, exhibited much higher catalytic activity than the 8-

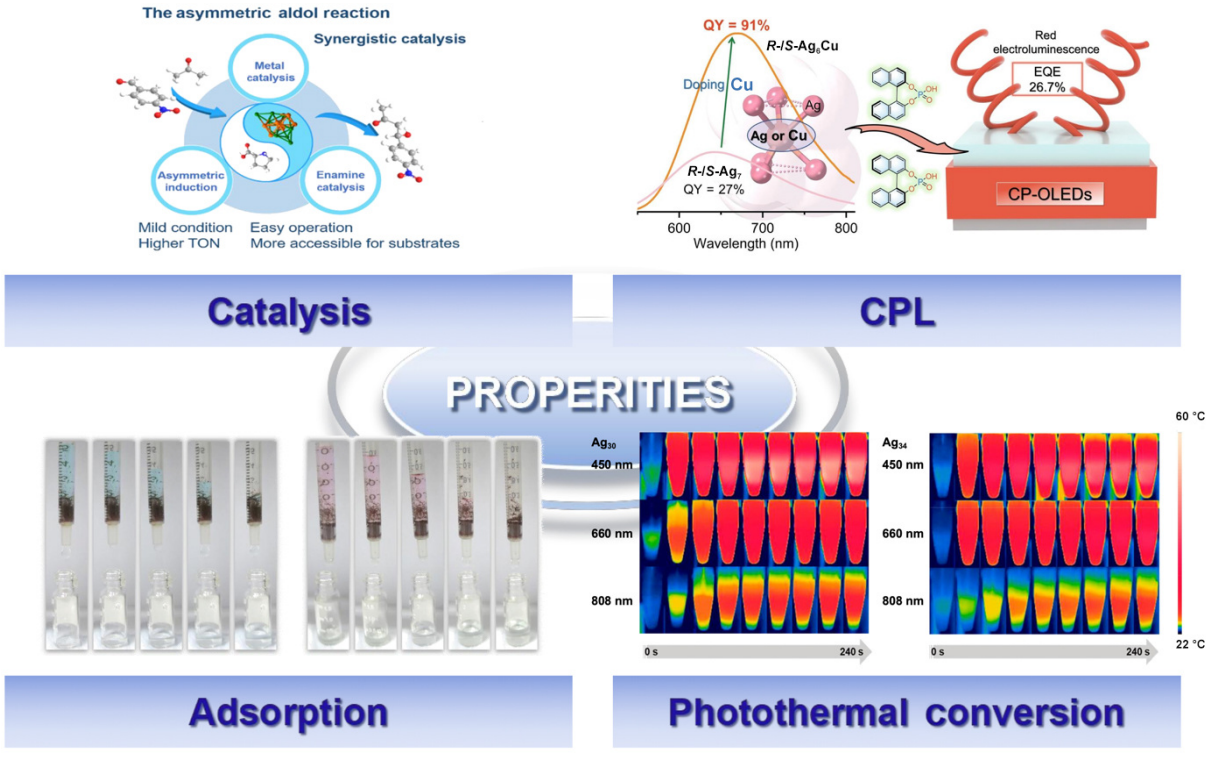

Figure 9 Catalysis, CPL, adsorption and photothermal conversion properties of nanoclusters protected by O donor ligands. Reproduced with permission from Ref. [56, 79], © American Chemical Society 2023; Ref. [67], © Wiley-VCH GmbH 2024; Ref. [76], © Gupta, R. K. et al. 2023.

electron **Ag_{21}-2**. Although both clusters provide sufficient space for 4-NP adsorption, the closed-shell electronic structure of Ag_{21} is less favorable for 4-NP adsorption. It is therefore possible that the difference in catalytic performance between the two Ag_{21} clusters arises from their different adsorption strengths toward the substrate.

***L-/D*-Au_7Ag_8** reported in 2023 was used in asymmetric Aldol reactions [56]. Experimental results demonstrated that incorporating proline ligands into metal nanoclusters considerably enhanced catalytic efficiency. Under identical conditions, the turnover number (TON) per ***L-/D*-Au_7Ag_8** cluster reached 72 within 5 h. Each cluster contains six pyrrolidine sites, corresponding to a TON of 12 per catalytic site, which is approximately three times higher than that of pure proline and six times higher than a proline–Ag complex. The enhanced catalysis arises from the synergistic interaction between the metal core and proline, while the surface arrangement of proline on ***L-/D*-Au_7Ag_8** further improves substrate accessibility at the catalytic sites.

Furthermore, Yang and Lv reported a POM-protected silver cluster catalyst for the CO_2 reduction reaction (CO_2RR) [95]. In a CO_2-degassed reaction solution, the catalyst system composed of $[Ru(bpy)_3(TEOA)]$ (bpy = 2,2′-bipyridine; TEOA = triethanolamine) and $[Ag_{24}(Si_2W_{18}O_{66})_3]$ (**Ag_{24}-Si**) acted as an efficient photocatalytic CO_2 photosensitizer. Upon irradiation, triethanolamine was reduced to formic acid (HCO_2H) as the primary product (~ 23.3 μmol), with CO and H_2 as minor byproducts. The selectivity and TON for HCOOH production reached approximately 90% and 467.4, respectively. This study demonstrated that the POM-protected **Ag_{24}-Si** cluster exhibited high selectivity for CO_2 reduction to formic acid, highlighting its remarkable catalytic activity. Recently, they again constructed two Ag_{14} clusters ($[Ag_{14}(Sb_3W_{30})_2]$-1, **Ag_{14}-1**; $[Ag_{14}(Sb_3W_{30})_2]$-2, **Ag_{14}-2**) and used them to catalyze photocatalytic hydrogen evolution [97]. The synergistic interaction between the redox-active $[Sb_3W_{30}]$ ligands and the silver active sites enabled both clusters to efficiently catalyze hydrogen evolution, achieving TON values of ~ 24,117 and 22,233 after 6 h of photocatalysis. Notably, **Ag_{14}-1** exhibited superior stability compared to **Ag_{14}-2** because some catalysts partially decomposed to form POM-protected silver nanoparticles during the reaction.

3.2 Circularly polarized luminescence (CPL)

Introducing chirality into luminescent coinage-metal nanoclusters via chiral O-donor ligands is a highly effective strategy for producing nanoclusters with CPL properties [57, 64, 67, 98]. Zang and Dong assembled a series of materials using bridging ligands and ***R-/S*-Ag_{20}** clusters protected by a chiral acid ligand (*R-/S*-THF-COOH) to achieve highly efficient CPL (Table 1) [98]. They observed that these materials could rapidly transform from a single CPL band at room temperature to well-separated dual CPL emissions at low temperature. The CPL spectra mirrored the trend of photoluminescence (PL), indicating effective chirality transfer between the chiral ligands and the luminescent cluster core. The luminescent dissymmetry factor (g_{lum}) of these nanoclusters reaches values as low as 1×10^{-3}, demonstrating notable CPL performance.

In 2025, Chen's group used the phosphonate ligand BNDHP to construct a silver cluster enantiomer (***R-/S*-Ag_7**) and a silver–copper cluster enantiomer (***R-/S*-Ag_6Cu**), and investigated their CPL and circularly polarized electroluminescence properties [67]. Compared with ***R-/S*-Ag_7**, the incorporation of Cu(I) atoms not only increases the luminescence quantum yield of ***R-/S*-Ag_6Cu** by a factor of three—by accelerating intersystem crossing and reverse intersystem crossing processes—but also renders the alloy cluster structure more rigid owing to stronger Ag–Cu interactions. In addition to

Table 1 Comparison of CPL properties of other clusters with O donor ligands protected nanoclusters

Compound	PLQY	g_{lum}	State	Ref.
***L*-/*D*-CF351**	—	5×10^{-3}	Solid	[57]
***R*-/*S*-Ag_{12n}**	50.3%	1.2×10^{-2}	Solution ($CHCl_3$)	[64]
***R*-/*S*-Ag_6Cu**	91.8%/90.3%	7×10^{-4}	Solution (CH_2Cl_2)	[67]
	11.8%/13.1%	1.1×10^{-3}	Solid	
***R*-/*S*-Ag_{20}**	—	1×10^{-3}	Solid	[98]
***R*-/*S*-Cu_{14}**	8.2%	3×10^{-3}	Solid	[99]
	1.6%	1×10^{-2}	Solution (DCM:hexane = 1:9)	
***R*-/*S*-Ag_{17}**	8.0%	1.2×10^{-3}	Solid	[100]
***R*-/*S*-$Au_{12}Ag_{32}$**	8.0%	6×10^{-3}	Solution (DMAc)	[101]

considerably enhancing thermodynamic stability, the CPL asymmetry factor of ***R*-/*S*-Ag_6Cu** is doubled. Circularly polarized organic light-emitting diodes (CP-OLEDs) based on ***R*-/*S*-Ag_6Cu** were fabricated via a solution process and exhibited efficient circularly polarized electroluminescence, with a maximum external quantum efficiency of 26.7%, an electroluminescence asymmetry factor of $\pm 6 \times 10^{-4}$, and chiral optical properties consistent with those observed in photoluminescence.

3.3 Adsorption

Calixarene ligands, with their deep cavities, are promising materials for molecular adsorption. In 2023, Sun's group reported a silver cluster, $(CrO_4)_2Cl_6@Ag_{46}(PTC4A)_6(^iPrS)_{12}(CH_3CN)_6$ (**Ag_{46}**, PTC4A = *p*-phenylthiacalix[4]arene) and demonstrated its use in dye adsorption [76]. Three representative organic dyes—methyl orange (MO), methylene blue (MB), and rhodamine B (RhB)—were tested under dark conditions at room temperature, varying in charge and size. MB and RhB are cationic, while RhB is larger, and MO is anionic and similar in size to MB. Remarkably, only cationic dyes were adsorbed by **Ag_{46}**, likely owing to electrostatic interactions between the positively charged dyes and the negatively charged inner walls of the thiacalix[4]arene-coordinated cavity. This represents the first report of a metal nanocluster showing exceptional selectivity for cationic dyes in aqueous environments. The same group also constructed a **Cu_{12}** cluster ($[Cu_{12}(Cbz\text{-}PrA)_4(BTCA)_2]$, Cbz-PrAH = 9-(prop-2-yn-1-yl)-9H-carbazole) and explored its iodine adsorption capabilities [77]. Owing to its permanent porosity, **Cu_{12}** achieved 97.2% iodine removal within 60 min from aqueous solution, corresponding to a total uptake of 2.96 $g \cdot g^{-1}$, outperforming most reported iodine adsorbents. Moreover, the material exhibited notable recyclability because I_2**@Cu_{12}** could be regenerated by immersion in ethyl acetate and reused for subsequent adsorption cycles.

3.4 Photothermal conversion

Ligands containing aromatic rings can strongly absorb light, while silver cores, with their unique electronic properties and thermal characteristics, are well-suited for converting light into heat. Accordingly, a series of **Ag_8** clusters reported by Liu and coworkers in 2023 was used to investigate photothermal conversion arising from multiple π-disordered anthracene groups [50]. When exposed to light, the temperature of the four clusters in this study rapidly reaches its peak within 20 min, and four consecutive photothermal cycles can be performed without any loss of activity, demonstrating excellent stability and photothermal recyclability. The presence of multiple π-disordered anthracene groups on the cluster surface, along with free electrons within the $[Ag_8]^{6+}$ core, enables efficient intramolecular charge transfer, enhancing light absorption. This promotes the ligand-to-metal charge transfer quenching and subsequent photon emission, thereby optimizing photothermal conversion. Remarkably, the photothermal conversion performance of this series of nanoclusters exceeds that of all previously reported silver-based photothermal materials.

In 2024, Sun and Wang reported two silver clusters, $Ag_{30}(BTCA)_4(TBPMT)_8$ (**Ag_{30}**, TBPMT = 4-tert-butylbenzenemethanethiol) and $Ag_{34}Na_4Cl_4(BTCA)_4(TBPMT)_{14}(EtOH)_4$ (**Ag_{34}**) [79]. This study evaluated the photothermal conversion performance of **Ag_{30}** and **Ag_{34}** in chloroform solutions under laser irradiation at various wavelengths. Both clusters exhibited considerable temperature increases at 450 and 660 nm. Photothermal conversion efficiencies, calculated from cooling curves, were 41.07% (450 nm) and 34.58% (660 nm) for **Ag_{30}**, and 34.99% (450 nm) and 22.82% (660 nm) for **Ag_{34}**, with all values remaining stable over six experimental cycles. The stability of these clusters is attributed to the solvent-controlled kernel formation during the reduction process and the saturation coordination pattern of fully deprotonated H_4BTCA toward Ag atoms.

4 Conclusions

In summary, O-donor ligands have shown great promise in stabilizing metal nanoclusters. Their negative charges and unique geometries make them particularly effective for precisely tuning the surface chemistry of nanoclusters. Such fine control over the metal–ligand interface provides a strong foundation for designing nanoclusters with enhanced performance in applications such as catalysis and adsorption, by optimizing electron transfer, reactant binding, and other key processes. As a result, the on-demand synthesis of metal nanoclusters with tailored properties and diverse applications becomes increasingly feasible. Looking ahead, several directions for further exploration of O-donor protection in coinage-metal nanoclusters could help advance this field:

(1) Carboxylate, sulfonate, phosphinate, and phosphonate ligands are among the earliest and most widely used O-donor ligands in coinage-metal nanocluster chemistry, yet they generally exhibit relatively weak coordination strength. Moreover, phenolates have not been successfully used in the assembly of metal clusters, despite their aromatic frameworks being advantageous for stabilizing metal complexes and clusters. Therefore, the key challenge lies in enhancing the binding affinities of O-donor ligands through rational tuning of the electronic effects of substituents on these ligands.

(2) While ligands containing one or a few O-donor groups are most common, ligands with multiple O-donor sites are attracting increasing attention. For example, Liu et al. reported an **Ag_8** nanocluster stabilized by the dicarboxylate ligand pfga in 2020 [41]. Another notable example is calixarene, a class of rigid macrocyclic phenolate oligomers with tunable cavities and multiple coordination sites, which allows accurate construction and functionalization of metal nanoclusters. This highlights the potential of carefully selecting and arranging the binding sites of multidentate O-donor ligands. A higher density of coordination sites considerably enhances their capacity to stabilize complex metal cores. Rational design of such ligands provides a route to structural innovation beyond classical archetypes and offers opportunities for tailoring cluster properties.

清華大学出版社 Tsinghua University Press | SciOpen

(3) POMs are promising stabilizing ligands for metal nanoclusters owing to their structural diversity and intrinsic properties. By carefully designing the spatial arrangement of donor atoms in POM ligands, metal precursors can be guided to undergo oriented nucleation and growth. This strategy enables the synthesis of previously inaccessible, high-nuclearity architectures with unique structures and properties, opening new opportunities for advanced applications.

(4) Analysis of existing clusters indicates that functional groups attached to O-donor ligands considerably influence cluster structures, affecting features such as chiral centers, luminescence, and polycyclic conjugated systems. Future research should focus on exploiting the unique surface chemistry and enhanced stability provided by these ligands. Such functionalization is expected to increase the number of active sites, fine-tune surface hydrophilicity and lipophilicity, and critically modulate molecular adsorption and activation. These effects are likely to enhance key performance metrics of metal nanoclusters across diverse applications, including catalysis, photocatalysis, CPL, and adsorption-based separation technologies.

Overall, the use of O-donor ligands to stabilize metal nanoclusters has long been recognized. These ligands show great potential for enabling novel structures and properties in coinage-metal nanoclusters, yet their value remains underappreciated. We hope this review will highlight the importance of O-donor ligands in constructing metal–oxygen interfaces in nanoclusters. Continued research in this area is likely to yield considerable advances in structural control and functional tuning of metal nanoclusters. The future of O-donor ligands as versatile passivating agents in cluster chemistry appears exceptionally promising.

Data availability

All data needed to support the conclusions in the paper are presented in the manuscript. Additional data related to this paper may be requested from the corresponding author upon request.

Acknowledgements

This work was supported by the National Natural Science Foundation of China (Nos. 22371044, 22442035, 22571075, 22561038, 22531004, and 92361301) and the Science Foundation of the Fujian Province, China (No. 2025J01436).

Declaration of competing interest

The authors have no competing interests to declare that are relevant to the content of this article. Author Quan-Ming Wang is the guest editor of this special issue, but he is not involved in the peer-review or decision of this article.

Author contribution statement

J.-J. L.: Data curation, visualization, writing – original draft. Y.-Y. L.: Data curation. Y.-N. Y.: Data curation. W.-T. L.: Data curation. Z.-J. G.: Resources, supervision, writing – review & editing. K.-G. L.: Resources, supervision, writing – review & editing. Q.-H. W.: Resources, supervision, writing – review & editing. Z. L.: Conceptualization, resources, supervision, project administration, writing – review & editing. Q.-M. W.: resources, supervision, writing – review & editing. All the authors have approved the final manuscript.

Use of AI statement

None.

References

[1] Xu, Q. H.; Gong, X. K.; Zhao, Z. X.; Wang, L.; Sun, J.; He, J. L.; Li, S. M.; Shen, H. Comprehensive and practical guidelines for reduction synthesis of atomically precise coinage-metal nanoclusters. *Polyoxometalates* **2025**, *4*, 9140075.

[2] Shi, W. Q.; Zeng, L. L.; He, R. L.; Han, X. S.; Guan, Z. J.; Zhou, M.; Wang, Q. M. Near-unity NIR phosphorescent quantum yield from a room-temperature solvated metal nanocluster. *Science* **2024**, *383*, 326–330.

[3] Lei, Z.; Pei, X. L.; Guan, Z. J.; Wang, Q. M. Full Protection of intensely luminescent gold(I)-silver(I) cluster by phosphine ligands and inorganic anions. *Angew. Chem., Int. Ed.* **2017**, *56*, 7117–7120.

[4] Wang, G. L.; Huang, T.; Murray, R. W.; Menard, L.; Nuzzo, R. G. Near-IR luminescence of monolayer-protected metal clusters. *J. Am. Chem. Soc.* **2005**, *127*, 812–813.

[5] Hu, J. H.; Li, Y. M.; Zhang, B.; Kang, X.; Zhu, M. Z. Atomically precise nanocluster-catalyzed coupling reactions. *Inorg. Chem. Front.* **2024**, *11*, 4974–5003.

[6] Langille, M. R.; Zhang, J.; Personick, M. L.; Li, S. Y.; Mirkin, C. A. Stepwise evolution of spherical seeds into 20-fold twinned icosahedra. *Science* **2012**, *337*, 954–957.

[7] Zhang, Q. B.; Xie, J. P.; Yang, J. H.; Lee, J. Y. Monodisperse icosahedral Ag, Au, and Pd nanoparticles: Size control strategy and superlattice formation. *ACS Nano* **2009**, *3*, 139–148.

[8] Hu, F.; Yang, G. Y.; Zheng, L. M.; Liang, G. J.; Wang, Q. M. Deciphering icosahedra structural evolution with atomically precise silver nanoclusters. *Science* **2025**, *389*, 921–924.

[9] Pei, X. L.; Yang, Y.; Lei, Z.; Chang, S. S.; Guan, Z. J.; Wan, X. K.; Wen, T. B.; Wang, Q. M. Highly active gold(I)-silver(I) oxo cluster activating sp^3 C–H bonds of methyl ketones under mild conditions. *J. Am. Chem. Soc.* **2015**, *137*, 5520–5525.

[10] Teo, B. K.; Shi, X. B.; Zhang, H. Pure gold cluster of 1: 9: 9: 1: 9: 9: 1 layered structure: A novel 39-metal-atom cluster $[(Ph_3P)_{14}Au_{39}Cl_6]Cl_2$ with an interstitial gold atom in a hexagonal antiprismatic cage. *J. Am. Chem. Soc.* **1992**, *114*, 2743–2745.

[11] McPartlin, M.; Mason, R.; Malatesta, L. Novel cluster complexes of gold(0)-gold(I). *J. Chem. Soc. D* **1969**, 334–334.

[12] Wan, X. K.; Yuan, S. F.; Lin, Z. W.; Wang, Q. M. A chiral gold nanocluster Au_{20} protected by tetradentate phosphine ligands. *Angew. Chem., Int. Ed.* **2014**, *53*, 2923–2926.

[13] Yuan, S. F.; Li, J. J.; Guan, Z. J.; Lei, Z.; Wang, Q. M. Ultrastable hydrido gold nanoclusters with the protection of phosphines. *Chem. Commun.* **2020**, *56*, 7037–7040.

[14] Yan, J. Z.; Malola, S.; Hu, C. Y.; Peng, J.; Dittrich, B.; Teo, B. K.; Häkkinen, H.; Zheng, L. S.; Zheng, N. F. Co-crystallization of atomically precise metal nanoparticles driven by magic atomic and electronic shells. *Nat. Commun.* **2018**, *9*, 3357.

[15] Zeng, C. J.; Chen, Y. X.; Liu, C.; Nobusada, K.; Rosi, N. L.; Jin, R. C. Gold tetrahedra coil up: Kekulé-like and double helical superstructures. *Sci. Adv.* **2015**, *1*, e1500425.

[16] Yang, H. Y.; Wang, Y.; Lei, J.; Shi, L.; Wu, X. H.; Mäkinen, V.; Lin, S. C.; Tang, Z. C.; He, J.; Häkkinen, H. et al. Ligand-stabilized $Au_{13}Cu_x$ (x = 2, 4, 8) bimetallic nanoclusters: Ligand engineering to control the exposure of metal sites. *J. Am. Chem. Soc.* **2013**, *135*, 9568–9571.

[17] Xu, Y.; Pu, Y.; Zhang, Q.; Kang, X.; Zhu, M. Z. Order-by-order control over the nonlinear optical properties of atomically precise nanoclusters. *Chin. J. Struct. Chem.* **2025**, *44*, 100735.

[18] Lei, Z.; Wan, X. K.; Yuan, S. F.; Guan, Z. J.; Wang, Q. M. Alkynyl approach toward the protection of metal nanoclusters. *Acc. Chem.*

Res. **2018**, *51*, 2465–2474.

[19] Zeng, J. L.; Guan, Z. J.; Du, Y.; Nan, Z. A.; Lin, Y. M.; Wang, Q. M. Chloride-promoted formation of a bimetallic nanocluster $Au_{80}Ag_{30}$ and the total structure determination. *J. Am. Chem. Soc.* **2016**, *138*, 7848–7851.

[20] Hu, F.; Li, J. J.; Guan, Z. J.; Yuan, S. F.; Wang, Q. M. Formation of an alkynyl-protected Ag_{112} silver nanocluster as promoted by chloride released *in situ* from CH_2Cl_2. *Angew. Chem., Int. Ed.* **2020**, *59*, 5312–5315.

[21] Zhao, H.; Zhang, C. K.; Han, B. L.; Wang, Z.; Liu, Y. C.; Xue, Q. W.; Tung, C. H.; Sun, D. Assembly of air-stable copper(I) alkynide nanoclusters assisted by tripodal polydentate phosphoramide ligands. *Nat. Synth.* **2024**, *3*, 517–526.

[22] Albright, E. L.; Levchenko, T. I.; Kulkarni, V. K.; Sullivan, A. I.; DeJesus, J. F.; Malola, S.; Takano, S.; Nambo, M.; Stamplecoskie, K.; Häkkinen, H. et al. N-heterocyclic carbene-stabilized atomically precise metal nanoclusters. *J. Am. Chem. Soc.* **2024**, *146*, 5759–5780.

[23] Lei, Z.; Endo, M.; Ube, H.; Shiraogawa, T.; Zhao, P.; Nagata, K.; Pei, X. L.; Eguchi, T.; Kamachi, T.; Ehara, M. et al. N-Heterocyclic carbene-based C-centered Au(I)-Ag(I) clusters with intense phosphorescence and organelle-selective translocation in cells. *Nat. Commun.* **2022**, *13*, 4288.

[24] Ube, H.; Zhang, Q.; Shionoya, M. A carbon-centered hexagold(I) cluster supported by N-heterocyclic carbene ligands. *Organometallics* **2018**, *37*, 2007–2009.

[25] Yuan, S. F.; Liu, W. D.; Liu, C. Y.; Guan, Z. J.; Wang, Q. M. Nitrogen donor protection for atomically precise metal nanoclusters. *Chem.—Eur. J.* **2022**, *28*, e202104445.

[26] Yuan, S. F.; Xu, C. Q.; Li, J.; Wang, Q. M. A ligand-protected golden fullerene: The dipyridylamido Au_{32}^{8+} nanocluster. *Angew. Chem., Int. Ed.* **2019**, *58*, 5906–5909.

[27] Hu, F.; Luyang, H. W.; He, R. L.; Guan, Z. J.; Yuan, S. F.; Wang, Q. M. Face-centered cubic silver nanoclusters consolidated with tetradentate formamidinate ligands. *J. Am. Chem. Soc.* **2022**, *144*, 19365–19371.

[28] Jiang, W. Y.; Wei, J. Y.; Liu, K. G. Atomically precise superatomic silver nanoclusters stabilized by O-donor ligands. *Chin. J. Struct. Chem.* **2024**, *43*, 100371.

[29] Greiser, T.; Weiss, E. Kristallstruktur des Kupfer(I)-tert-butoxids, $[(CH_3)_3COCu]_4$. *Chem. Ber.* **1976**, *109*, 3142–3146.

[30] Aalten, H. L.; Van Koten, G.; Goubitz, K.; Stam, C. H. A stable trinuclear mixed (organic)(organo)copper cluster: Synthesis and structure of bis(benzoato)(mesity)tricopper(I). *J. Chem. Soc. Chem. Commun.* **1985**, *1985*, 1252–1253.

[31] Zhao, X. L.; Wang, Q. M.; Mak, T. C. W. Self-assembled silver polyhedra with embedded acetylide dianion stabilized by perfluorocarboxylate and 4-hydroxyquinoline ligands. *Inorg. Chem.* **2003**, *42*, 7872–7876.

[32] Wang, Q. M.; Mak, T. C. W. Crown ethers as ancillary ligands in the assembly of silver(I) aggregates containing embedded acetylenediide. *Chem.—Eur. J.* **2003**, *9*, 43–50.

[33] Wang, Q. M.; Mak, T. C. W. Facile construction of anionic silver(I) aggregates with embedded acetylide and cyanide ions. *Angew. Chem., Int. Ed.* **2002**, *41*, 4135–4137.

[34] Wang, Q. M.; Mak, T. C. W. Crown-ether-directed assembly of discrete and one-dimensional silver aggregates containing embedded acetylenediide. *Angew. Chem., Int. Ed.* **2001**, *40*, 1130–1133.

[35] Wang, Q. M.; Mak, T. C. W. Argentophilicity and solvent-induced structural diversity in double salts of silver acetylide with silver perfluoroalkyl carboxylates. *J. Am. Chem. Soc.* **2001**, *123*, 7594–7600.

[36] Reger, D. L.; Huff, M. F.; Wolfe, T. A.; Adams, R. D. A novel copper(I) complex with bridging alkyne ligands. The synthesis and structural characterization of $[Cu_4(O_2CCF_3)_4(\mu\text{-EtC}{\equiv}CEt)_2]$. *Organometallics* **1989**, *8*, 848–850.

[37] Reiß, P.; Weigend, F.; Ahlrichs, R.; Fenske, D. $[\{Ag(^tBuNH_2)_2\}_4][\{Ag(^tBuNH_2)(^tBuN{=}CHCH_3)\}_2][Ag_{12}(CF_3CO_2)_{14}]$: A compound with an Ag_{12}^{8+} cluster core. *Angew. Chem., Int. Ed.* **2000**, *39*, 3925–3929.

[38] Huang, R. W.; Wei, Y. S.; Dong, X. Y.; Wu, X. H.; Du, C. X.; Zang, S. Q.; Mak, T. C. W. Hypersensitive dual-function luminescence switching of a silver-chalcogenolate cluster-based metal-organic framework. *Nat. Chem.* **2017**, *9*, 689–697.

[39] Zhang, L. L. M.; Mak, T. C. W. Temperature-mediated template release: Facile growth of copper(I) mixed ethynediide/isopropylethynide nanoclusters. *Angew. Chem., Int. Ed.* **2017**, *56*, 16228–16232.

[40] Wen, Z. R.; Guan, Z. J.; Zhang, Y.; Lin, Y. M.; Wang, Q. M. $[Au_7Ag_9(dppf)_3(CF_3CO_2)_7BF_4]_n$: A linear nanocluster polymer from molecular Au_7Ag_8 clusters covalently linked by silver atoms. *Chem. Commun.* **2019**, *55*, 12992–12995.

[41] Liu, K. G.; Gao, X. M.; Liu, T. Y.; Hu, M. L.; Jiang, D. E. All-carboxylate-protected superatomic silver nanocluster with an unprecedented rhombohedral Ag_8 core. *J. Am. Chem. Soc.* **2020**, *142*, 16905–16909.

[42] Chai, J. S.; Yang, S.; Chen, T.; Li, Q. Z.; Wang, S. X.; Zhu, M. Z. Chiral inversion and conservation of clusters: A case study of racemic $Ag_{32}Cu_{12}$ nanocluster. *Inorg. Chem.* **2021**, *60*, 9050–9056.

[43] Sun, J.; Sun, F.; Tang, J. Q.; Tang, X. K.; Wu, Q. Y.; Huo, R.; He, A.; Sachurilatu; Sun, X. L.; Chaolumen et al. Carboxylate engineering for manipulating the optical and assembly properties of copper clusters. *Inorg. Chem. Front.* **2023**, *10*, 2618–2625.

[44] Su, Y. M.; Liu, W.; Wang, Z.; Wang, S. A.; Li, Y. A.; Yu, F.; Zhao, Q. Q.; Wang, X. P.; Tung, C. H.; Sun, D. Benzoate-induced high-nuclearity silver thiolate clusters. *Chem.—Eur. J.* **2018**, *24*, 4967–4972.

[45] Li, J. J.; Liu, C. Y.; Guan, Z. J.; Lei, Z.; Wang, Q. M. Anion-directed regulation of structures and luminescence of heterometallic clusters. *Angew. Chem., Int. Ed.* **2022**, *61*, e202201549.

[46] Yan, B. Z.; You, X. X.; Tang, X. K.; Sun, J.; Xu, Q. H.; Wang, L.; Guan, Z. J.; Li, F. Y.; Shen, H. Carboxylate-protected "isostructural" Cu_{20} nanoclusters as a model system: Carboxylate effect on controlling catalysis. *Chem. Mater.* **2024**, *36*, 1004–1012.

[47] Wang, Z.; Su, H. F.; Tung, C. H.; Sun, D.; Zheng, L. S. Deciphering synergetic core-shell transformation from $[Mo_6O_{22}@Ag_{44}]$ to $[Mo_8O_{28}@Ag_{50}]$. *Nat. Commun.* **2018**, *9*, 4407.

[48] Gao, X. M.; Bigdeli, F.; Wang, H. H.; Hanifehpour, Y.; Esrafili, L.; Li, J. Z.; Wang, W.; Liu, K. G.; Cai, X. Q.; Morsali, A. Facile synthesis of two new hexa-/octa-nuclear silver clusters and investigation of their optical features. *Polyhedron* **2021**, *194*, 114940.

[49] Liu, J. W.; Wang, Z.; Chai, Y. M.; Kurmoo, M.; Zhao, Q. Q.; Wang, X. P.; Tung, C. H.; Sun, D. Core modulation of 70-nuclei core-shell silver nanoclusters. *Angew. Chem., Int. Ed.* **2019**, *58*, 6276–6279.

[50] Wang, H. H.; Wei, J. Y.; Bigdeli, F.; Rouhani, F.; Su, H. F.; Wang, L. X.; Kahlal, S.; Halet, J. F.; Saillard, J. Y.; Morsali, A. et al. Monocarboxylate-protected two-electron *superatomic* silver nanoclusters with high photothermal conversion performance. *Nanoscale* **2023**, *15*, 8245–8254.

[51] Zhang, Z. X.; Dai, J. F.; Feng, C. C.; Shi, C. H.; Zhou, L. B.; Yu, X. Y.; Yang, C.; Zhang, X. J.; Yang, H. Y. From intermediate capture to functional cluster construction: Synthesis of silver clusters and their Br^-/I^- sensing applications. *Polyoxometalates* **2025**, *4*, 9140086.

[52] Akhbari, K.; Morsali, A.; Zhu, L. G. Thermal, fluorescence, solution and structural studies of one-dimensional Ag^I coordination polymer with Ag–Ag and Ag-π interactions. *J. Mol. Struct.* **2008**, *891*, 132–137.

[53] Liang, M. X.; Ruan, C. Z.; Sun, D.; Kong, X. J.; Ren, Y. P.; Long, L. S.; Huang, R. B.; Zheng, L. S. Solvothermal Synthesis of Four Polyoxometalate-Based Coordination Polymers Including Diverse Ag(I)···π Interactions. *Inorg. Chem.* **2014**, *53*, 897–902.

[54] Liu, Q. X.; Wu, Y. L.; Feng, M.; Chen, W. M.; Zheng, Z. P. Rare silver-histidine cluster complex and its single-crystal-to-single-

crystal phase-transition behavior. *ACS Omega* **2022**, *7*, 8141–8149.
[55] Liu, W. D.; Wang, J. Q.; Yuan, S. F.; Chen, X.; Wang, Q. M. Chiral superatomic nanoclusters Ag_{47} induced by the ligation of amino acids. *Angew. Chem., Int. Ed.* **2021**, *60*, 11430–11435.
[56] Wang, J. Q.; He, R. L.; Liu, W. D.; Feng, Q. Y.; Zhang, Y. E.; Liu, C. Y.; Ge, J. X.; Wang, Q. M. Integration of metal catalysis and organocatalysis in a metal nanocluster with anchored proline. *J. Am. Chem. Soc.* **2023**, *145*, 12255–12263.
[57] Li, S.; Yan, Z. P.; Li, X. L.; Kong, Y. J.; Li, H. Y.; Gao, G. G.; Zheng, Y. X.; Zang, S. Q. Stepwise achievement of circularly polarized luminescence on atomically precise silver clusters. *Adv. Sci.* **2020**, *7*, 2000738.
[58] Li, S.; Du, X. S.; Li, B.; Wang, J. Y.; Li, G. P.; Gao, G. G.; Zang, S. Q. Atom-precise modification of silver(I) thiolate cluster by shell ligand substitution: A new approach to generation of cluster functionality and chirality. *J. Am. Chem. Soc.* **2018**, *140*, 594–597.
[59] Gupta, A. K.; Kishore, P. V. V. N.; Liao, J. H.; Chen, Y. J.; Liu, C. W. Hexadecanuclear copper monothiocarbonates: An emissive cluster building block. *Eur. J. Inorg. Chem.* **2017**, *2017*, 1989–1993.
[60] Wang, Q. M.; Mak, T. C. W. Novel honeycomb-like layered structure: The first isomorphous triple salts of silver acetylide. *J. Am. Chem. Soc.* **2000**, *122*, 7608–7609.
[61] Ai, P.; Danopoulos, A. A.; Braunstein, P.; Monakhov, K. Y. A novel, rigid diphosphine with an active NHC spacer; di- and trinuclear complexes of d^{10} coinage metals. *Chem. Commun.* **2014**, *50*, 103–105.
[62] Wang, Z.; Su, H. F.; Kurmoo, M.; Tung, C. H.; Sun, D.; Zheng, L. S. Trapping an octahedral Ag_6 kernel in a seven-fold symmetric Ag_{56} nanowheel. *Nat. Commun.* **2018**, *9*, 2094.
[63] Wang, Z.; Su, H. F.; Wang, X. P.; Zhao, Q. Q.; Tung, C. H.; Sun, D.; Zheng, L. S. Johnson solids: Anion-templated silver thiolate clusters capped by sulfonate. *Chem.—Eur. J.* **2018**, *24*, 1640–1650.
[64] Wang, J. Y.; Si, Y. B.; Luo, X. M.; Wang, Z. Y.; Dong, X. Y.; Luo, P.; Zhang, C.; Duan, C. Y.; Zang, S. Q. Stepwise amplification of circularly polarized luminescence in chiral metal cluster ensembles. *Adv. Sci.* **2023**, *10*, 2207660.
[65] Guan, Z. J.; He, R. L.; Yuan, S. F.; Li, J. J.; Hu, F.; Liu, C. Y.; Wang, Q. M. Ligand engineering toward the trade-off between stability and activity in cluster catalysis. *Angew. Chem., Int. Ed.* **2022**, *61*, e202116965.
[66] Wei, J. Y.; Bigdeli, F.; Wang, L. X.; Hou, L. L.; Panjehpour, A.; Ma, Y.; Wang, K. Z.; Morsali, A.; Liu, K. G. Template-free synthesis of two new luminescent one-dimensional high-nuclearity silver polyclusters. *Inorg. Chem.* **2023**, *62*, 10185–10192.
[67] Ding, X. Y.; Shi, L. X.; Wang, J. Y.; Xu, L. J.; Zhang, L. Y.; Chen, Z. N. Doping copper(I) in Ag_7 cluster for circularly polarized OLEDs with external quantum efficiency of 26.7%. *Angew. Chem., Int. Ed.* **2025**, *64*, e202417934.
[68] Jin, J. L.; Xie, Y. P.; Cui, H.; Duan, G. X.; Lu, X.; Mak, T. C. W. Structure-directing role of phosphonate in the synthesis of high-nuclearity silver(I) sulfide-ethynide-thiolate clusters. *Inorg. Chem.* **2017**, *56*, 10412–10417.
[69] Fang, J. J.; Liu, Z.; Shen, Y. L.; Xie, Y. P.; Lu, X. Template-assisted synthesis of isomeric copper(I) clusters with tunable structures showing photophysical and electrochemical properties. *Chem. Sci.* **2023**, *14*, 12637–12644.
[70] Su, Y. M.; Su, H. F.; Wang, Z.; Li, Y. A.; Schein, S.; Zhao, Q. Q.; Wang, X. P.; Tung, C. H.; Sun, D.; Zheng, L. S. Three silver nests capped by thiolate/phenylphosphonate. *Chem.—Eur. J.* **2018**, *24*, 15096–15103.
[71] Su, Y. M.; Wang, Z.; Schein, S.; Tung, C. H.; Sun, D. A keplerian Ag_{90} nest of Platonic and Archimedean polyhedra in different symmetry groups. *Nat. Commun.* **2020**, *11*, 3316.
[72] Yuan, Z. R.; Wang, Z.; Han, B. L.; Zhang, C. K.; Zhang, S. S.; Zhu, Z. Y.; Yu, J. H.; Li, T. D.; Li, Y. Z.; Tung, C. H. et al. Ag_{22} nanoclusters with thermally activated delayed fluorescence protected by Ag/cyanurate/phosphine metallamacrocyclic monolayers through *in-situ* ligand transesterification. *Angew. Chem., Int. Ed.* **2022**, *61*, e202211628.
[73] Guan, Z. J.; Zeng, J. L.; Nan, Z. A.; Wan, X. K.; Lin, Y. M.; Wang, Q. M. Thiacalix[4]arene: New protection for metal nanoclusters. *Sci. Adv.* **2016**, *2*, e1600323.
[74] Guan, Z. J.; Hu, F.; Yuan, S. F.; Nan, Z. A.; Lin, Y. M.; Wang, Q. M. The stability enhancement factor beyond eight-electron shell closure in thiacalix[4]arene-protected silver clusters. *Chem. Sci.* **2019**, *10*, 3360–3365.
[75] Wang, Z.; Su, H. F.; Gong, Y. W.; Qu, Q. P.; Bi, Y. F.; Tung, C. H.; Sun, D.; Zheng, L. S. A hierarchically assembled 88-nuclei silver-thiacalix[4]arene nanocluster. *Nat. Commun.* **2020**, *11*, 308.
[76] Gupta, R. K.; Li, L.; Wang, Z.; Han, B. L.; Feng, L.; Gao, Z. Y.; Tung, C. H.; Sun, D. Regulating the assembly and expansion of the silver cluster from the Ag_{37} to Ag_{46} nanowheel driven by heteroanions. *Chem. Sci.* **2023**, *14*, 1138–1144.
[77] Zhang, C. K.; Wang, Z.; Si, W. D.; Chu, H. X.; Zhou, L.; Li, T.; Huang, X. Q.; Gao, Z. Y.; Azam, M.; Tung, C. H. et al. Dynamic and transformable Cu_{12} cluster-based C–H···π-stacked porous supramolecular frameworks. *Nat. Commun.* **2023**, *14*, 6413.
[78] Zheng, L. M.; Shi, W. Q.; Hu, F.; Guan, Z. J.; Wang, Q. M. All-calixarene-protected silver nanocluster with all silver atoms in a face-centered cubic arrangement. *J. Am. Chem. Soc.* **2024**, *146*, 25101–25107.
[79] Wang, Z.; Zhao, H.; Li, Y. Z.; Zhang, C. K.; Gupta, R. K.; Tung, C. H.; Sun, D. Thiacalix[4]arene-protected silver nanoclusters encapsulating different two-electron superatom oligomers. *Nano Lett.* **2024**, *24*, 458–465.
[80] Li, S. Q.; Li, L. J.; Tian, Y. Q.; Mu, W. L.; Meng, R. X.; Yan, J.; Liu, C. Synthesis and characterization of Ag(I) alkynyl nanoclusters utilizing Mo^{VI}-anchored thiacalix[4]arene metalloligands: Application in electrocatalytic CO_2 reduction. *Polyoxometalates* **2024**, *3*, 9140038.
[81] Zhao, X. L.; Zhang, L. P.; Mak, T. C. W. Polyhedral $C_2@Ag_n$ cages distorted by ancillary pyridine *N*-oxideligands in silver-acetylenediide complexes. *Dalton Trans.* **2006**, 3141–3146.
[82] Li, B.; Huang, R. W.; Qin, J. H.; Zang, S. Q.; Gao, G. G.; Hou, H. W.; Mak, T. C. W. Thermochromic luminescent nest-like silver thiolate cluster. *Chem.—Eur. J.* **2014**, *20*, 12416–12420.
[83] Tamgho, I. S.; Crandall, L. A.; Engle, J. T.; Ziegler, C. J. The synthesis of a silver hexagon using a diiminoisoindoline-based ligand. *Inorg. Chem. Commun.* **2017**, *76*, 122–124.
[84] Qu, M.; Zhang, F. Q.; Wang, D. H.; Li, H.; Hou, J. J.; Zhang, X. M. Observation of non-FCC copper in alkynyl-protected Cu_{53} nanoclusters. *Angew. Chem., Int. Ed.* **2020**, *59*, 6507–6512.
[85] Ge, R.; Cai, P. W.; Sun, C.; Sun, Y. Q.; Li, X. X.; Zheng, S. T. Development of non-closed silver clusters by transition-metal-coordination-cluster substituted polyoxometalate templates. *Chem. Sci.* **2024**, *15*, 12543–12549.
[86] Gupta, A. K.; Orthaber, A. Serendipitous and targeted synthesis of high nuclearity clusters—Carbonate and oxalate encapsulating silver alkynides. *Cryst. Growth Des.* **2020**, *20*, 4232–4237.
[87] Lei, Z.; Chang, S. S.; Wang, Q. M. Vapochromic gold(I)-silver(I) cluster protected by alkynyl and phosphine ligands. *Eur. J. Inorg. Chem.* **2017**, *2017*, 5098–5102.
[88] Hou, L. L.; Bigdeli, F.; Cheng, X.; Wang, L. X.; Zhang, J. W.; Liu, K. G.; Morsali, A. Synthesis of two neutral silver alkynyl nanoclusters by a single divalent tetrahedral anion template and a study of their optical features. *Inorg. Chem.* **2022**, *61*, 16693–16698.
[89] Schneider, S.; Roberts, J. A. S.; Salata, M. R.; Marks, T. J. Mixed diketonate thiolate copper(I) precursors for materials synthesis: Control of Cu_2S-forming thermolysis pathways by manipulating lewis acid and base cluster building blocks. *Angew. Chem., Int. Ed.* **2006**, *45*, 1733–1736.
[90] Jin, J. L.; Shen, Y. L.; Xie, Y. P.; Lu, X. Silver ethynide clusters constructed with fluorinated β-diketonate ligands. *CrystEngComm* **2018**, *20*, 2036–2042.

[91] Kikukawa, Y.; Kuroda, Y.; Yamaguchi, K.; Mizuno, N. Diamond-shaped $[Ag_4]^{4+}$ cluster encapsulated by silicotungstate ligands: Synthesis and catalysis of hydrolytic oxidation of silanes. *Angew. Chem., Int. Ed.* **2012**, *51*, 2434–2437.
[92] Yonesato, K.; Ito, H.; Itakura, H.; Yokogawa, D.; Kikuchi, T.; Mizuno, N.; Yamaguchi, K.; Suzuki, K. Controlled assembly synthesis of atomically precise ultrastable silver nanoclusters with polyoxometalates. *J. Am. Chem. Soc.* **2019**, *141*, 19550–19554.
[93] Yonesato, K.; Ito, H.; Yokogawa, D.; Yamaguchi, K.; Suzuki, K. An ultrastable, small $\{Ag_7\}^{5+}$ nanocluster within a triangular hollow polyoxometalate framework. *Angew. Chem., Int. Ed.* **2020**, *59*, 16361–16365.
[94] Yonesato, K.; Yanai, D.; Yamazoe, S.; Yokogawa, D.; Kikuchi, T.; Yamaguchi, K.; Suzuki, K. Surface-exposed silver nanoclusters inside molecular metal oxide cavities. *Nat. Chem.* **2023**, *15*, 940–947.
[95] Feng, Y. Q.; Fu, F. Y.; Zeng, L. L.; Zhao, M. Y.; Xin, X.; Liang, J. K.; Zhou, M.; Fang, X. K.; Lv, H. J.; Yang, G. Y. Atomically precise silver clusters stabilized by lacunary polyoxometalates with photocatalytic CO_2 reduction activity. *Angew. Chem., Int. Ed.* **2024**, *63*, e202317341.
[96] Kamachi, M.; Yonesato, K.; Okazaki, T.; Yanai, D.; Kikkawa, S.; Yamazoe, S.; Ishikawa, R.; Shibata, N.; Ikuhara, Y.; Yamaguchi, K. et al. Synthesis of a gold-silver alloy nanocluster within a ring-shaped polyoxometalate and its photocatalytic property. *Angew. Chem., Int. Ed.* **2024**, *63*, e202408358.
[97] Chi, M. Z.; Wei, J. Y.; Zhao, Z. C.; Liu, X. Y.; Sun, W. T.; Feng, Y. Q.; Lv, H. J.; Yang, G. Y. Structural isomerism of $\{Ag_{14}\}^{10+}$ nanocluster encapsulated by bowl-like polyoxometalates. *Angew. Chem., Int. Ed.* **2025**, *64*, e202424499.
[98] Wang, J. Y.; Yuan, J. W.; Liu, X. M.; Liu, Y. J.; Bai, F.; Dong, X. Y.; Zang, S. Q. Engineering intelligent chiral silver cluster-assembled materials for temperature-triggered dynamic circularly polarized luminescence. *Aggregate* **2024**, *5*, e508.
[99] Zhang, M. M.; Dong, X. Y.; Wang, Z. Y.; Li, H. Y.; Li, S. J.; Zhao, X. L.; Zang, S. Q. AIE triggers the circularly polarized luminescence of atomically precise enantiomeric copper(I) alkynyl clusters. *Angew. Chem., Int. Ed.* **2020**, *59*, 10052–10058.
[100] Zhang, M. M.; Dong, X. Y.; Wang, Z. Y.; Luo, X. M.; Huang, J. H.; Zang, S. Q.; Mak, T. C. W. Alkynyl-stabilized superatomic silver clusters showing circularly polarized luminescence. *J. Am. Chem. Soc.* **2021**, *143*, 6048–6053.
[101] Kong, Y. J.; Hu, J. H.; Dong, X. Y.; Si, Y. B.; Wang, Z. Y.; Luo, X. M.; Li, H. R.; Chen, Z. W.; Zang, S. Q.; Mak, T. C. W. Achiral-core-metal change in isomorphic enantiomeric $Ag_{12}Ag_{32}$ and $Au_{12}Ag_{32}$ clusters triggers circularly polarized phosphorescence. *J. Am. Chem. Soc.* **2022**, *144*, 19739–19747.

Jia-Jing Lan received her B.E. (2020) and M.Sc. (2024) from College of Chemical Engineering and College of Chemistry, Fuzhou University, respectively. She is now pursuing her PhD of Inorganic Chemistry at the same university under the supervision of Prof. Zhen Lei. Her research is mainly focused on the synthesis, structure, and properties of atomically precise coinage metal nanoclusters stabilized by oxygen donor ligands.

Yao-Yao Lian graduated from Henan University with a BS in Chemistry in 2024. Currently, she is pursuing a Master's degree in the research group of Associate Professor Zong-Jie Guan at Hunan University. Her research focuses on the synthesis of photoactive silver nanoclusters and their catalytic properties.

Ya-Nan Yang graduated from Henan Agricultural University with a B.S. in Applied Chemistry in 2024. She is now a Master's student in the group of Prof. Qiao-Hua Wei at the College of Chemistry, Fuzhou University. Her research interest is controlled synthesis and properties of ligand-protected copper clusters.

Wen-Ting Liu is a Master's student at the College of Chemistry, Fuzhou University. She is now studying in the group of Prof. Zhen Lei, working on gold clusters with circularly polarized luminescence (CPL) and other properties.

Zong-Jie Guan graduated from Hunan University with a BS in Chemistry in 2013. After obtaining his PhD in Physical Chemistry from Xiamen University in 2019, he conducted postdoctoral research at Tsinghua University under the supervision of Prof. Quan-Ming Wang. Currently, he is a researcher at College of Chemistry and Chemical Engineering, Hunan University. His research interests focus mainly on the synthesis and applications of metal nanoclusters and cluster-based cages.

Kuan-Guan Liu Ph.D. is a Professor at School of Materials and New Energy, Ningxia University. He earned his Ph.D. from Xiamen University (2015) and was a visiting scholar at Nanjing University (2018–2019). His research focuses on Cu/Ag cluster-based functional materials for catalysis, smart optical devices, photothermal desalination, and 3D printing. He has published over 50 papers in leading journals including *J. Am. Chem. Soc*. and Nat. Commun., holds 6 authorized patents, and was named a Top 2% Global Scientist (2025).

Qiao-Hua Wei is a Research Professor at College of Chemistry, Fuzhou University, and a Minjiang Science Communication Scholar in Fujian Province. She earned her Ph.D. in Inorganic Chemistry from the Fujian Institute of Research on the Structure of Matter, Chinese Academy of Sciences in 2006. She subsequently advanced her research as a postdoctoral fellow at the University of Sheffield, United Kingdom (2006–2007), supported by the prestigious Royal Society of Chemistry (RSC) Scholarship. Since being recruited to Fuzhou University as an Overseas High-Level Talent in 2007, she has established and leads a focused research program dedicated to coinage metal cluster-based photoelectric materials and energy devices. Prof. Qiao-Hua Wei's scholarly output and innovation include more than 90 peer-reviewed research articles in international chemistry and materials journals. In addition, she holds 8 authorized Chinese invention patents.

Zhen Lei is a Research Professor at Fuzhou University. He graduated from Huazhong University of Science and Technology (HUST) with a B.S. in Applied Chemistry and B.A. in German in 2009. During 2009–2018, he studied and worked in Prof. Quan-Ming Wang's group as graduated student, PhD candidate, research assistant, and postdoc at Xiamen University and Tsinghua University, respectively. His Ph.D. of Science in Physical Chemistry was obtained from Xiamen University in 2015. From 2018 to 2023, he worked in Prof. Mitsuhiko Shionoya's Lab at The University of Tokyo as a Project Researcher and then Project Assistant Professor. He joined the College of Chemistry, Fuzhou University in 2023, under the supports of NSFC overseas program and Minjiang Scholar program of Fujian Province. His main research interests lie in ligand-protected coinage metal complexes/clusters/nanoclusters.

Quan-Ming Wang is a professor at Tsinghua University. He received BS and MS degrees from Xiamen University in 1989 and 1992, respectively. During 1992-1998, he worked at Fujian Institute of Research on the Structure of Matter, Chinese Academy of Sciences. He received PhD degree from The Chinese University of Hong Kong in 2001. He conducted postdoctoral research at University of Rochester and University of California at Riverside. He joined Xiamen University as a full professor in 2005 and moved to Tsinghua University in 2015. His research interests include metal cluster chemistry and cluster-based nanoscience.